Chapter 6

Results and Discussion

6. Results and Discussion

6. 1.Characterization of Synthesized Compounds

The compounds were rationally designed after analysis and comprehensive of literature review for antimicrobial and anti-malarial activity and were prepared by coupling of substituted benzaldehydes with respective cyclopentanone/cyclohexanone and cycloheptanone (in ratio of 2: 1) in a base catalyzed Claisen-Schmidt condensation where temperature was maintained between 15-25˚C. The reaction mixture was further refluxed (15-20h) with hydrazines (hydrazine hydrate, phenyl-hydrazine) and acetic acid.

The progress of reactions and purity were monitored by thin layer chromatography (TLC) on pre-coated Merck alu-foil plate (silica gel 60F-254, 0.25 mm thickness). The compounds were obtained in good yield (48 - 86%). Melting points were determined on a Veego capillary melting point apparatus and are uncorrected. FT-IR spectra were recorded on KBr pellets on Shimadzu FT-IR spectrophotometer. ^{1}H NMR spectra were recorded on a Bruker 300 MHz spectrophotometer. All NMR spectra were obtained in deuterated chloroform (CDCl$_3$); chemical shifts are reported in parts per million, and coupling constants in Hertz (Hz). Multiplicities are reported as follows: s (singlet), d (doublet), t (triplet), m (multiplet). Mass spectra were recorded on a LC-MS-2010A spectrometer on ESI positive mode and molecular ion peaks are reported as m/z ratio. Elemental analysis of synthesized compounds was recorded on EXETER-CE-440 elemental analyzer.

The FT-IR spectra of curcumin analogues showed absorption bands in the range of 1567 (C=N) and 1232 (C–N) for these groups. 3502 (O-H), 1582 (C=N), 1467 (C=C),the absorption bands in the range of 1506 - 1583 cm^{-1} appeared for aromatic C=C. The broad bands of phenolic OH in some compounds appeared in the range of 3402 - 3541 cm^{-1}. The nuclear magnetic resonance (^{1}H NMR) spectra of the compounds were recorded in DMSO-d_6 and CDCl$_3$ solvents and the structural assignments are given in physico-chemical and analytical data details. The NMR spectrum of curcumin analogues (A1-B5, CP1-CP14 & C1-C15) showed sharp singlet at δ 6.31- 6.91 indicating the presence of methylene (-CH) proton. The appearance of multiplets at δ 6.9 - 7.3 was due to aromatic protons.

In the mass spectrum, molecular ion peak, base peak and fragmentation peaks appeared. For compound A1 a peak of m/z: 331 (M+1)$^+$ appeared which is in conformity with the molecular formula C$_{22}$H$_{22}$N$_2$O.For compound CP1 a peak of m/z: 317 (M+1)$^+$ appeared which is in conformity with the molecular formula C$_{21}$H$_{20}$N$_2$O.For compound C1 a peak of m/z: 345 (M+1)$^+$ appeared which is in conformity with the molecular formula

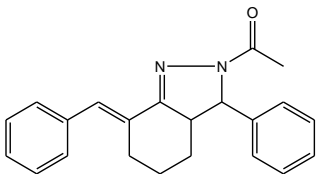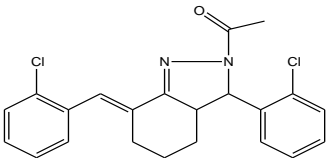$C_{21}H_{20}N_2O$. Similarly others compounds showed peak at m/z which matches with their molecular formula.

All the curcumin analogues gave C, H, and N analyses within ± 0.4 % of the theoretical values. The FT-IR, ^{1}H NMR, ^{13}C NMR, Mass spectral data and elemental analysis results are in agreement with the proposed structures.
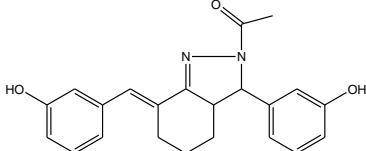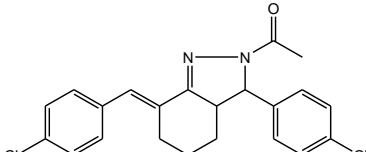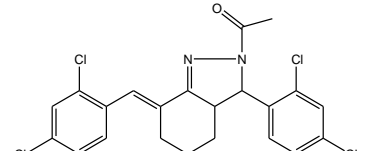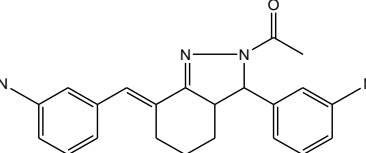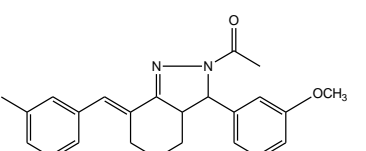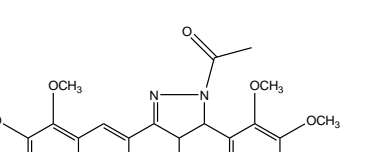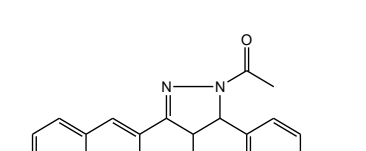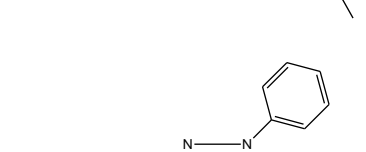
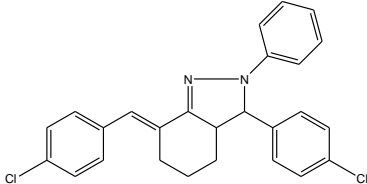## 6.1.1 Synthesis and characterization of Hexahydroindazole analogues of curcumin (A1-B5)
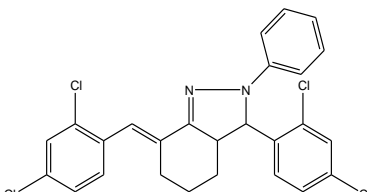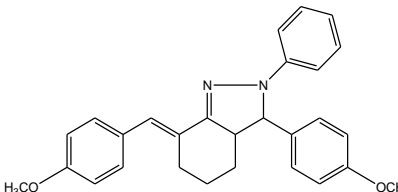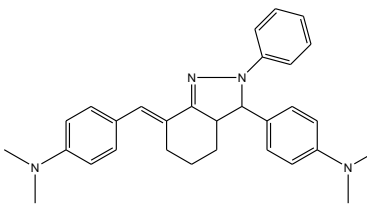
These were prepared in two steps. In First step, respective dibenzylidiene cyclohexanones were synthesized. A mixture of ethanol (20ml) and sodium hydroxide solution (10%, 10 ml) was taken in a beaker, maintained at temperature between 15 to 25ºC. The solution was vigorously stirred and one half of the previously prepared mixture of appropriate aromatic aldehyde and cyclohexanone (in ratio of 2:1) was added to it. After 20 min, the remaining of the aromatic aldehyde-cyclohexanone mixture was added. The reaction mixture was further stirred for 45 minutes. The solid was filtered off, washed with distilled water, and subjected to further purification by recrystallization with ethyl alcohol

In second step, the substituted dibenzylidene cyclohexanone (1.2 mmol) obtained from first step was dissolved in glacial acetic acid (5 mL), and hydrazine hydrate/ phenylhydrazine (1.5 mmol) was added to the solution. The solution was refluxed for 12 hours and monitored by TLC .The solvent was removed in vacuum and the residue was recrystallized with ethyl alcohol.

Table 6.1. Physical properties of Hexahydroindazole analogues of curcumin

Code	Structure	Solubility	Melting point (ºC)	Percentage yield (%)	R_f value
A1		Chloroform	90-92	75.00	0.52
A2		Chloroform	102-104	87.00	0.53

A3		Chloroform	166-168	71.00	0.49
A4		Chloroform	126-128	50.00	0.39
A5		Chloroform	152-154	76.00	0.56
A6		Chloroform	130-132	59.00	0.56
A7		Chloroform	110-112	76.00	0. 42
A8		Chloroform	210-212	87.00	0.46
A9		Chloroform	150-152	71.00	0.51
B1		Chloroform	58-60	67.00	0.46

B2		Chloroform	78-80	48.00	0.51
B3		Chloroform	70-72	65.00	0.52
B4		Chloroform	80-82	73.00	0.48
B5		Chloroform	178-180	85.00	0.56

Spectral data for hexahydroindazole analogues of curcumin

Compound A1:*(E)-1-(7-benzylidene-3-phenyl-3,3a,4,5,6,7-hexahydro-2H-indazol-2-yl) ethanone*

Yellow powder.

^{1}H NMR (CDCl$_3$, 300 MHz, 25 °C): 7.61-7.25 (m, 10H), 6.31 (s, 1H, =CH), 4.72 (d, 1H), 2.67 (m, 1H), 2.12 (s, 3H, CH$_3$), 1.81-1.42 (m, 6H).

^{13}C NMR (CDCl$_3$, 75 MHz, 25 °C): 166.9, 154.4, 141.7, 136.0, 134.9, 131.9, 128.5, 127.6, 127.1, 127.9, 126.3, 70.2, 41.8, 27.5, 24.8, 23.7.

ESI-MS: m/z: 331 (M+1)$^+$

Elemental analysis found (Calc.) for C$_{22}$H$_{22}$N$_2$O: C, 79.97 (79.65); H, 6.71 (6.73); N, 8.48(8.45).

Compound A2:*(E)-1-(7-(2-chlorobenzylidene)-3-(2-chlorophenyl)-3, 3a, 4, 5, 6, 7 hexahydro-2H-indazol-2-yl)ethanone*

Yellow powder.

^{1}H NMR (CDCl$_3$, 300 MHz, 25 °C): 7.72-7.20 (m, 8H), 6.69 (s, 1H, =CH), 4.5 (d, 1H), 2.67 (m, 1H), 2.02 (s, 3H, CH$_3$), 1.85-1.43 (m, 6H).

^{13}C NMR (CDCl$_3$, 75 MHz, 25 °C): 166.5, 154.6, 141.5, 136.5 134.7, 133.5, 133.1, 130.7, 129.5, 129.3, 129.3, 128.2, 127.1, 127.0, 126.6, 126.4, 65.9, 42.4, 23.3.

ESI-MS: m/z: 400 (M+1)$^+$

Elemental analysis found (Calc.) for C$_{22}$H$_{20}$Cl$_2$N$_2$O: C, 66.17(66.43); H, 5.05(5.03); N, 7.02(7.30)

Compound A3:*(E)-1-(7-(3-hydroxybenzylidene)-3-(3-hydroxyphenyl)-3,3a,4,5,6,7-hexahydro-2H-indazol-2-yl)ethanone*

Yellow powder.

^{1}H NMR (CDCl$_3$, 300 MHz, 25 °C): 7.52-6.51 (m, 8 H), 6.31 (s, 1H, =CH), 5.30 (s, 2H), 4.6 (d, 1H), 2.55 (m, 1H), 2.32 (s, 3H, CH$_3$), 1.75-1.37 (m, 6H).

^{13}C NMR (CDCl$_3$, 75 MHz, 25 °C): 167.2, 158.9, 156.6, 155.5, 140.7, 135.6, 135.1, 131.7, 130.4, 129.7, 121.8, 120.4, 115.6, 113.4, 113.2, 22.2.

ESI-MS: m/z: 363 (M+1)$^+$

Elemental analysis found (Calc.) for C$_{22}$H$_{22}$N$_2$O$_3$: C, 72.91(72.71); H,6.12 (6.09); N, 7.73(7.76)

Compound A4:*(E)-1-(7-(4-chlorobenzylidene)-3-(4-chlorophenyl)-3,3a,4,5,6,7-hexahydro-2H-indazol-2-yl)ethanone*

Yellow powder.

^{1}H NMR (CDCl$_3$, 300 MHz, 25 °C): 7.66-7.58 (m,8 H), 6.27 (s, 1H, =CH), 4.2 (d, 1H), 2.65 (m, 1H), 2.01 (s, 3H, CH$_3$), 1.77-1.45 (m, 6H).

^{13}C NMR (CDCl$_3$, 75 MHz, 25 °C): 168.5, 155.6, 139.7, 136.0, 133.3, 131.5, 129.0, 128.6, 128.4, 70.9, 42.8, 27.8, 24.5, 21.4.

ESI-MS: m/z: 400(M+2)$^+$

Elemental analysis found (Calc.) for C$_{22}$H$_{20}$ Cl$_2$N$_2$O: C, 63.62(63.36); H,4.85 (4.86); N,6.75 (6.77)

Compound A5:*(E)-1-(7-(2,4-dichlorobenzylidene)-3-(2,4-dichlorophenyl)-3,3a,4,5,6,7-hexahydro-2H-indazol-2-yl)ethanone*

Yellow powder.

^{1}H NMR (CDCl$_3$, 300 MHz, 25 °C): 7.71-7.02 (m, 6H), 6.56 (s, 1H, =CH), 4.7 (d, 1H), 2.66 (m, 1H), 2.02 (s, 3H, CH$_3$), 1.85-1.23 (m, 6H).

^{13}C NMR (CDCl$_3$, 75 MHz, 25 °C): 163.5, 152.6, 150.1, 137.6, 136.8, 132.4, 132.1, 131.4, 131.0, 130.3, 127.9, 126.8, 126.5, 125.2, 120.8, 75.8, 42.1, 27.9, 24.3, 23.1.

ESI-MS: m/z: 469(M+1)$^+$

Elemental analysis found (Calc.) for C$_{22}$H$_{18}$ Cl$_4$N$_2$O: C, 56.44(56.66); H,3.88 (3.83); N, 5.98 (5.96)

Compound A6:*(E)-1-(7-(3-nitrobenzylidene)-3-(3-nitrophenyl)-3,3a,4,5,6,7-hexahydro-2H-indazol-2-yl) ethanone*

Yellow powder.

^{1}H NMR (CDCl$_3$, 300 MHz, 25 °C): 8.29-7.54 (m, 8H), 6.42 (s, 1H, =CH), 4.4 (d, 1H), 2.63 (m, 1H), 2.02 (s, 3H, CH$_3$), 1.81-1.43 (m, 6H).

^{13}C NMR (CDCl$_3$, 75 MHz, 25 °C): 167.5, 154.6, 146.8, 146.2, 140.4, 136.1, 135.3, 134.6, 134.2, 129.5, 129.3, 128.7, 123.8, 122.7, 121.7, 120.7, 69.7, 42.8, 27.8, 24.5, 23.4.

ESI-MS: 421(M+1)$^+$

Elemental analysis found (Calc.) for C$_{22}$H$_{20}$ N$_4$O$_5$: C, 62.85(62.60); H,4.79 (4.80); N, 13.33(13.28)

Compound A7:*(E)-1-(7-(3-methoxybenzylidene)-3-(3-methoxyphenyl)-3,3a,4,5,6,7-hexahydro-2H-indazol-2-yl)ethanone*

Yellow powder.

^{1}H NMR (CDCl$_3$, 300 MHz, 25 °C): 7.49-6.21 (m,8 H), 6.11 (s, 1H, =CH), 4.1 (d, 1H), 3.75 (s, 6H), 2.68 (m, 1H), 2.04 (s, 3H, CH$_3$), 1.78 -1.32 (m, 6H).

^{13}C NMR (CDCl$_3$, 75 MHz, 25 °C): 169.5, 161.5, 160.4, 155.6, 142.5, 136.0, 134.8, 128.6, 126.5, 120.8, 120.4, 112.5, 112.0, 111.5, 71.2, 55.8, 42.8, 27.1, 24.5, 23.4.

ESI-MS: m/z: 391(M+1)$^+$

Elemental analysis found (Calc.) for C$_{24}$H$_{26}$N$_2$O$_3$: C, 73.82(73.63); H, 6.71(6.72); N, 7.17(7.16)

Compound A8:*(E)-1-(7-(2,3,4-trimethoxybenzylidene)-3-(2,3,4-trimethoxyphenyl)-3,3a,4,5,6,7-hexahydro-2H-indazol-2-yl)ethanone*

Yellow powder.

^{1}H NMR (CDCl$_3$, 300 MHz, 25 °C): 7.47 -6.25 (m,4 H), 6.59 (s, 1H, =CH), 4.4 (d, 1H), 3.75 (s,2x9H), 2.68 (m, 1H), 2.04 (s, 3H, CH$_3$), 1.80-1.35 (m, 6H). ^{13}C NMR (CDCl$_3$, 75 MHz, 25 °C): 168.5, 156.8, 155.9, 152.9, 151.1, 149.1, 142.3, 141.6, 136.0, 135.7, 132.7,

122.7, 121.4, 119.6, 108.2, 106.8, 104.7, 65.3, 61.7, 60.8, 60.3, 56.1, 43.1, 27.8, 24.5, 23.4.

ESI-MS: m/z: 511(M+1)$^+$

Elemental analysis found (Calc.) for $C_{28}H_{34}N_2O_7$: C, 65.87(65.92); H, 6.71(6.70); N, 5.49(5.48)

Compound A9:*(E)-1-(7-(4-(dimethylamino)benzylidene)-3-(4-(dimethylamino)phenyl)-3,3a,4,5,6,7-hexa hydro-2H-indazol-2-yl)ethanone*

Yellow powder.

^{1}H NMR (CDCl$_3$, 300 MHz, 25 °C): 7.64 -6.56 (m,8 H), 6.25 (s, 1H, =CH), 4.7 (d, 1H), 3.78 (s, 12 H), 2.68 (m, 1H), 2.54 (s, 3H, CH$_3$), 1.81-1.36 (m, 6H).

^{13}C NMR (CDCl$_3$, 75 MHz, 25 °C): 167.5, 154.6, 151.3, 149.3, 133.7, 132.1, 131.4, 128.7, 124.7, 112.7, 111.7, 72.9, 41.3, 26.8, 24.5, 23.4.

ESI-MS: m/z: 417 (M+1)$^+$

Elemental analysis found (Calc.) for $C_{26}H_{32}N_4O$: C, 74.97(74.96); H, 7.74(7.72); N, 13.45(13.43)

Compound B1:*(E)-7-(3-chlorobenzylidene)-3-(3-chlorophenyl)-2-phenyl-3,3a,4,5,6,7-hexahydro-2H-indazole*

Yellow powder.

^{1}H NMR (CDCl$_3$, 300 MHz, 25 °C): 7.34-6.75 (m, 13 H), 6.24 (s, 1H, =CH), 3.7 (d, 1H), 2.25 (m, 1H), 1.78-1.43 (m, 6H).

^{13}C NMR (CDCl$_3$, 75 MHz, 25 °C): 145.6, 143.8, 140.9, 136.0, 134.9, 134.2, 134.1, 130.0, 129.9, 129.5, 128.0, 126.9, 126.2, 119.7, 62.6, 40.5, 26.8, 24.8, 23.5.

ESI-MS: m/z: 434(M+1)$^+$

Elemental analysis found (Calc.) for $C_{26}H_{22}Cl_2N_2$: C, 72.06(71.97); H, 5.12(5.11); N, 6.46(6.52)

Compound B2:*(E)-7-(4-chlorobenzylidene)-3-(4-chlorophenyl)-2-phenyl-3,3a,4,5,6,7-hexahydro-2H-indazole*

Yellow powder.

^{1}H NMR (CDCl$_3$, 300 MHz, 25 °C): 7.78-6.73 (m, 13 H), 6.23 (s, 1H, =CH), 3.5 (d, 1H), 2.26 (m, 1H), 1.82-1.41 (m, 6H).

^{13}C NMR (CDCl$_3$, 75 MHz, 25 °C): 154.6, 143.8, 138.6, 136.0, 133.5, 133.3, 131.7, 131.5, 129.0, 129.5, 128.6, 128.4, 116.7, 63.1, 42.9, 28.6, 27.8, 24.8, 24.5.

ESI-MS: m/z: 434(M+1)$^+$

Elemental analysis found (Calc.) for $C_{26}H_{22}Cl_2N_2$: C, 72.20(73.37); H, 5.27(5.28); N, 6.10(6.11)

Compound B3: *(E)-7-(2,4-dichlorobenzylidene)-3-(2,4-dichlorophenyl)-2-phenyl-*

3,3a,4,5,6,7-hexahydro-2H-indazole

Yellow powder.

^{1}H NMR (CDCl$_3$, 300 MHz, 25 °C): 7.58-6.75 (m, 11H), 6.59 (s, 1H, =CH), 3.8 (d, 1H), 2.27 (m, 1H), 1.87-1.30 (m, 6H).

^{13}C NMR (CDCl$_3$, 75 MHz, 25 °C): 154.6, 150.5, 141.8, 138.6, 136.0, 133.8, 133.1, 131.7, 131.1, 130.3, 129.4, 128.9, 128.1, 126.7, 120.8, 116.7, 58.0, 41.4, 28.7, 24.5.

ESI-MS: m/z: 503(M+1)$^+$

Elemental analysis found (Calc.) for $C_{26}H_{20}Cl_4N_2$: C, 62.17(62.31); H, 4.01(4.02); N, 5.58(5.56)

Compound B4: *(E)-7-(4-methoxybenzylidene)-3-(4-methoxyphenyl)-2-phenyl-*

3,3a,4,5,6,7-hexahydro-2H-indazole

Yellow powder.

^{1}H NMR (CDCl$_3$, 300 MHz, 25 °C): 7.52-6.84 (m,13H), 6.32 (s, 1H, =CH), 3.5 (d, 1H), 3.73 (S, 6H), 2.25 (m, 1H), 1.84-1.42 (m, 6H).

^{13}C NMR (CDCl$_3$, 75 MHz, 25 °C): 158.8, 156.8, 144.8, 134.0, 131.8, 131.2, 130.2, 129.5, 127.8, 127.5, 121.8, 116.7, 113.2, 112.1, 63.1, 55.8, 42.9, 27.8, 24.8, 24.5.

ESI-MS: m/z: 425(M+1)$^+$

Elemental analysis found (Calc.) for $C_{28}H_{28}N_2O_2$: C, 79.22(79.43); H, 6.65(6.66); N, 6.60(6.62)

Compound B5: *(E)-4-(7-(4-(dimethylamino) benzylidene)-2-phenyl-3, 3a, 4, 5, 6, 7-*

hexahydro-2H-indazol-3-yl)-N,N-dimethylaniline

Yellow powder.

^{1}H NMR (CDCl$_3$, 300 MHz, 25 °C): 7.62-7.01 (m, 13 H), 6.24 (s, 1H, =CH), 3.1 (d, 1H), 3.07 (s, 12 H) 2.31 (m, 1H), 1.78 -1.20 (m, 6H).

^{13}C NMR (CDCl$_3$, 75 MHz, 25 °C): 154.2, 150.1, 146.3, 143.8, 136.7, 130.7, 130.4, 130.0, 129.7, 129.5,   128.9, 128.4, 127.1, 126.9, 116.7, 112.7, 111.7, 63.1, 42.9, 40.3, 27.8, 24.8, 24.5.
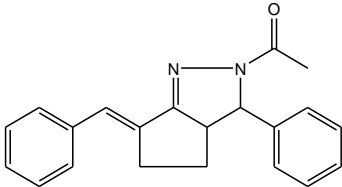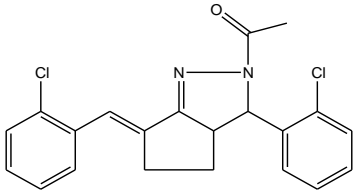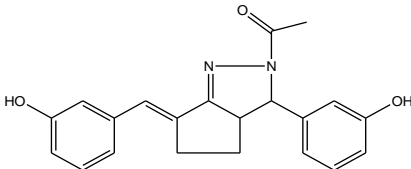
ESI-MS: m/z: 451 (M+1)$^+$

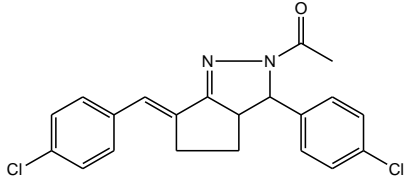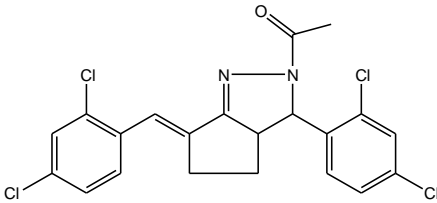Elemental analysis found (Calc.) for $C_{30}H_{34}N_4$: C, 79.96(80.02); H, 7.61(7.62); N, 12.43(12.41)
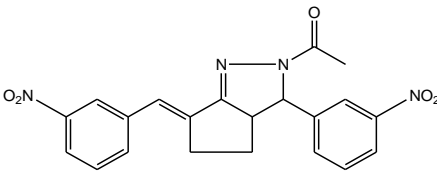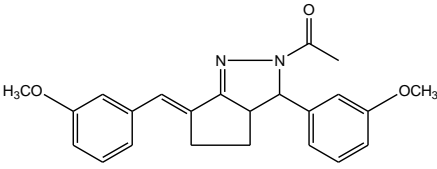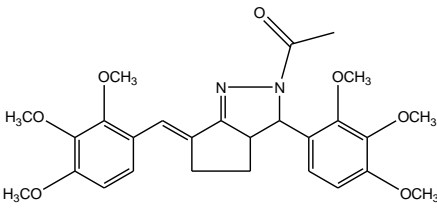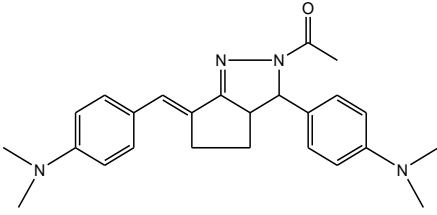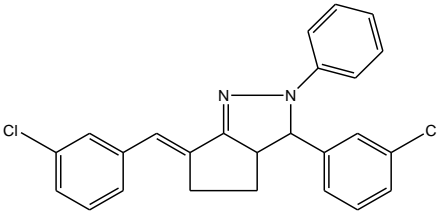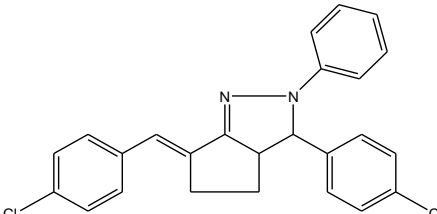
6.1.2. Synthesis and characterization of pyrazole analogues of curcumin (CP1-CP14)

These were prepared in two steps. In first step, respective dibenzylidiene cyclopentanones were synthesized. A mixture of ethanol (20 ml) and sodium hydroxide solution (10%, 10 ml) was taken in a beaker and was maintained at temperature between 15 to 25ºC. The solution was vigorously stirred and one half of previously prepared mixture of appropriate aromatic aldehyde and cyclopentanone (in molar ratio of 2: 1) was added to it. After 20 min, the remaining aromatic aldehyde-cyclopentanone mixture was added. The reaction mixture was further stirred for 45 minutes. The solid was filtered off, washed with distilled water, and subjected to further purification by crystallization with ethyl alcohol.

In second step, synthesized substituted dibenzylidene cyclopentanone (1.2 mmol) from first step was dissolved in glacial acetic acid (5 ml), and hydrazine hydrate (1.5 mmol) was added to the solution. The solution was refluxed for 14 hours and monitored by TLC. The solvent was removed in vacuum and the residue was crystallized with ethyl alcohol. The remaining analogues were also prepared by the same procedure.

Table 6.2. Physical properties of Pyrazole analogues of curcumin

Code	Structure	Solubility	Melting point (ºC)	Percentage yield (%)	Rf value
CP1		Chloroform	88-90	52.00	0.52
CP2		Chloroform	107-109	77.00	0.43
CP3		Chloroform	170-172	81.00	0.54

CP4		Chloroform	120-122	61.00	0.39
CP5		Chloroform	150-152	65.00	0.45
CP6		Chloroform	126-128	51.00	0.57
CP7		Chloroform	116-118	50.00	0. 50
CP8		Chloroform	208-210	48.00	0.58
CP9		Chloroform	146-148	75.00	0.52
CP10		Chloroform	70-72	68	0.55
CP11		Chloroform	76-78	54.00	0.51

CP12		Chloroform	86-88	67.00	0.54
CP13		Chloroform	92-94	73.00	071
CP14		Chloroform	94-96	65.00	0.61

Spectral data for pyrazole analogues of curcumin

Compound CP1: *(E)-1-(6-benzylidene-3-phenyl-3a,4,5,6, tertrahydrocyclopenta [c]pyrazol-2(3H)-yl) ethanone*

Yellow powder.

FT-IR (KBr, ν_{max}/cm^{-1}): 1567 (C=N), 1493 (C=C), 1232 (C–N).

^{1}H NMR (CDCl$_3$, 300 MHz, 25°C): 7.30 - 7.08 (m, 10H), 6.21 (s, 1H, =CH), 4.72 (d, 1H), 2.67 (m, 1H), 2.02 (s, 3H, -CH$_3$), 1.75 - 1.42 (m, 4H).

MS (ESI$^+$) m/z: 317(M+1)$^+$

Elemental analysis Calc. (found) for C$_{21}$H$_{20}$N$_2$O: C, 79.72 (79.75); H, 6.37 (6.39); N, 8.85 (8.82).

Compound CP2: *(E)-1-(6(2-chlorobenzylidene-3-(2-chlorophenyl)-3a,4,5,6-tertrahydrocyclopenta[c]pyrazol-2(3H)-yl)ethanone*

Yellow powder.

FT-IR (KBr, ν_{max}/cm^{-1}): 1586 (C=N), 1494 (C=C), 1234 (C–N).

^{1}H NMR (CDCl$_3$, 300 MHz, 25 °C): 7.22 - 7.05 (m, 8H), 6.69 (s, 1H, =CH), 4.5 (d, 1H), 2.67 (m, 1H), 2.02 (s, 3H, CH$_3$), 1.91-1.51 (m, 4H).

MS (ESI$^+$) m/z: 386(M+1)$^+$

Elemental analysis Calc. (found) for $C_{21}H_{18}Cl_2N_2O$: C, 65.46 (65.48); H, 4.71 (4.72); N, 7.27 (7.29).

Compound CP3: *(E)-1-(6(3-hydroxybenzylidene-3-(3-hydroxyphenyl)-3a,4,5,6-tertrahydrocyclopenta[c]pyrazol-2(3H)-yl)ethanone*

Yellow powder.

FT-IR (KBr, ν_{max}/cm^{-1}): 3502 (O-H), 1582 (C=N), 1467 (C=C), 1239 (C–N).

^{1}H NMR (CDCl$_3$, 300 MHz, 25°C): 7.04-6.51 (m, 8 H), 6.25 (s, 1H, =CH), 5.30 (s, 2H), 4.6 (d, 1H), 2.45 (m, 1H), 2.12 (s, 3H, CH$_3$), 2.01-1.2 (m, 4H).

MS (ESI$^+$) m/z: 349(M+1)$^+$

Elemental analysis Calc. (found) for $C_{21}H_{20}N_2O_3$: C, 72.40 (72.40); H, 5.79 (5.81); N, 8.04 (8.06).

Compound CP4: *(E)-1-(6(4-chlorobenzylidene-3-(4-chloroyphenyl)-3a,4,5,6-tertrahydrocyclopenta[c]pyrazol-2(3H)-yl)ethanone*

Yellow powder.

FT-IR (KBr, ν_{max}/cm^{-1}): 1596 (C=N), 1474 (C=C), 1244 (C–N).

^{1}H NMR (CDCl$_3$, 300 MHz, 25°C): 7.21 - 7.06 (m, 8 H), 6.27 (s, 1H, =CH), 4.5 (d, 1H), 2.65 (m, 1H), 2.01 (s, 3H, CH$_3$), 1.77-1.45 (m, 4H).

MS (ESI$^+$) m/z: 386(M+1)$^+$

Elemental analysis Calc. (found) for $C_{21}H_{18}Cl_2N_2O$: C, 65.46 (65.20); H, 4.71 (4.72); N, 7.27 (7.25).

Compound CP5: *(E)-1-(6(2,4-dichlorobenzylidene-3-(2,4-dichloroyphenyl)-3a,4,5,6-tertrahydrocyclopenta[c]pyrazol-2(3H)-yl)ethanone*

Yellow powder.

FT-IR (KBr, ν_{max}/cm^{-1}): 1576 (C=N), 1458 (C=C), 1249 (C–N).

^{1}H NMR (CDCl$_3$, 300 MHz, 25°C): 7.23 - 7.02 (m, 6H), 6.46 (s, 1H, =CH), 4.8 (d, 1H), 2.4 (m, 1H), 2.07 (s, 3H, CH$_3$), 2.01-1.24 (m, 4H).

MS (ESI$^+$) m/z: 455(M+1)$^+$

Elemental analysis Calc. (found) for $C_{21}H_{16}Cl_4N_2O$: C, 55.53 (55.31); H, 3.55 (3.56); N, 6.17 (6.19).

Compound CP6: *(E)-1-(6(3-nitrobenzylidene-3-(3-nitrophenyl)-3a,4,5,6-tertrahydrocyclopenta[c]pyrazol-2(3H)-yl)ethanone*

Yellow powder.

FT-IR (KBr, ν_{max}/cm^{-1}): 1596 (C=N), 1477 (C=C).

^{1}H NMR (CDCl$_3$, 300 MHz, 25 °C): 8.22 - 7.44 (m, 8H), 6.32 (s, 1H, =CH), 4.6 (d, 1H), 2.63 (m, 1H), 2.02 (s, 3H, CH$_3$), 2.04 - 1.23 (m, 4H).

MS (ESI$^+$) m/z: 407(M+1)$^+$

Elemental analysis Calc. (found) for C$_{21}$H$_{18}$N$_4$O$_5$: C, 62.06 (62.10); H, 4.46 (4.47); N, 13.79 (13.84).

Compound CP7: *(E)-1-(6(3-methoxybenzylidene-3-(3-methoxyphenyl)-3a,4,5,6-tertrahydrocyclopenta[c]pyrazol-2(3H)-yl)ethanone*

Yellow powder.

FT-IR (KBr, ν_{max}/cm^{-1}): 1584 (C=N), 1487 (C=C).

^{1}H NMR (CDCl$_3$, 300 MHz, 25°C): 7.15–6.52 (m, 8H), 6.11 (s, 1H, =CH), 4.1 (d, 1H), 2.05 (s, 3H), 2.48 (m, 1H), 3.70; 3.74 (s, 6H, 2OCH$_3$), 1.75–1.22 (m, 4H);

MS (ESI$^+$) m/z: 377 (M+1)$^+$.

Elemental analysis Calc. (found) for C$_{23}$H$_{24}$N$_2$O$_3$: C, 73.38 (73.40); H, 6.43 (6.41); N, 7.44 (7.45).

Compound CP8: *(E)-1-(6(2,3,4trimethoxybenzylidene-3-(2,3,4-trimethoxyphenyl)-3a,4,5,6-tertrahydrocyclopenta[c]pyrazol-2(3H)-yl)ethanone*

Yellow powder.

FT-IR (KBr, ν_{max}/cm^{-1}): 1577 (C=N), 1469 (C=C).

^{1}H NMR (CDCl$_3$, 300 MHz, 25°C): 7.21 - 6.20 (m, 4H), 6.49 (s, 1H, =CH), 4.2 (d, 1H), 2.01 (s, 3H), 2.68 (m, 1H), 3.65; 3.70; 3.75 (s, 18H, 6OCH$_3$), 1.70 - 1.15 (m, 4H).

MS (ESI$^+$) m/z: 497(M+1)$^+$.

Elemental analysis Calc. (found) for C$_{27}$H$_{32}$N$_2$O$_7$: C, 65.31 (65.57); H, 6.50 (6.52); N, 5.64 (5.60).

Compound CP9: *(E)-1-(6-(4-(dimethylamino)benzylidene)-3-(4dimethylaminophenyl)-3a,4,5,6tertrahydrocyclopenta[c]pyrazol-2(3H)-yl)ethanone*

Yellow powder.

FT-IR (KBr, ν_{max}/cm^{-1}): 3347 (=NH), 1596 (C=N), 1477 (C=C).

^{1}H NMR (CDCl$_3$, 300 MHz, 25°C): 7.14 - 6.46 (m, 8 H), 6.15 (s, 1H, =CH), 4.7 (d, 1H), 2.03 (s, 3H), 2.78; 2.80 (s, 12 H,N-CH$_3$ ×4), 2.68 (m, 1H), 1.75 - 1.26 (m, 4H).

MS (ESI$^+$) m/z: 403(M+1)$^+$

Elemental analysis Calc. (found) for $C_{25}H_{30}N_4O$: C, 74.59 (74.61); H, 7.51 (7.49); N, 13.92 (13.90).

Compound CP10: *(E)-6-(3-chlorobenzylidene)-3-(3-chlorophenyl)-2-phenyl-2,3,3a,4,5,6,-hexahydrocyclopenta[c]pyrazole*

Yellow powder.

FT-IR (KBr, v_{max}/cm^{-1}): 1566 (C=N), 1483 (C=C).

^{1}H NMR (CDCl$_3$, 300 MHz, 25 °C): 7.24-6.45 (m, 13 H), 6.20 (s, 1H, =CH), 3.50 (d, 1H), 2.21 (m, 1H), 1.75 - 1.23 (m, 4H).

MS (ESI$^+$) m/z: 418 (M)$^+$

Elemental analysis Calc. (found) for $C_{25}H_{20}Cl_2N_2$: C, 71.60 (71.66); H, 4.81 (4.82); N, 6.68 (6.70).

Compound CP11: *(E)-6-(4-chlorobenzylidene)-3-(4-chlorophenyl)-2-phenyl-2,3,3a,4,5,6,-hexahydrocyclopenta[c]pyrazole*

Yellow powder.

FT-IR (KBr, v_{max}/cm^{-1}): 1574 (C=N), 1484 (C=C).

^{1}H NMR (CDCl$_3$, 300 MHz, 25 °C): 7.28 - 6.13 (m, 13H), 6.03 (s, 1H, =CH), 3.50 (d, 1H), 2.26 (m, 1H), 1.62 - 1.21 (m, 4H).

MS (ESI$^+$) m/z: 419 (M)$^+$

Elemental analysis Calc. (found) for $C_{25}H_{20}Cl_2N_2$: C, 71.60 (71.75); H, 4.81 (4.84); N, 6.68 (6.70).

Compound CP12: *(E)-6-(2,4dichlorobenzylidene)-3-(2,4dichlorophenyl)-2-phenyl-2,3,3a,4,5,6,-hexahydrocyclopenta[c]pyrazole*

Yellow powder.

FT-IR (KBr, v_{max}/cm^{-1}): 1579 (C=N), 1450 (C=C).

^{1}H NMR (CDCl$_3$, 300 MHz, 25 °C): 7.28 - 6.05 (m, 11 H), 6.02 (s, 1H, =CH), 3.5 (d, 1H), 2.22 (m, 1H), 1.77-1.20 (m, 4H).

MS (ESI$^+$) m/z: 489(M+1)$^+$

Elemental analysis Calc. (found) for $C_{25}H_{18}Cl_4N_2$: C, 61.50 (61.47); H, 3.72 (3.78); N, 5.74 (5.72).

Compound CP13: *(E)-6-(4-methoxybenzylidene)-3-(4-methoxyphenyl)-2-phenyl-2,3,3a,4,5,6,-hexahydrocyclopenta[c]pyrazole*

Yellow powder.

FT-IR (KBr, ν_{max}/cm^{-1}): 1584 (C=N), 1496 (C=C).

^{1}H NMR (CDCl$_3$, 300 MHz, 25 °C): 7.22 - 6.14 (m, 13H), 6.11 (s, 1H, =CH), 3.5 (d, 1H), 3.68; 3.72 (s, 6H, 2OCH$_3$), 2.15 (m, 1H), 1.84 - 1.4 (m, 4H).

MS (ESI$^+$) m/z: 411 (M+1)$^+$

Elemental analysis Calc. (found) for C$_{27}$H$_{26}$N$_2$O$_2$: C, 79.00 (79.04); H, 6.38 (6.40); N, 6.82 (6.80).

Compound CP14: *(E)-4-(4-(dimethylamino) phenyl)-2-phenyl-3, 3a, 4, 5-tetrahydrocyclopenta[c] pyrazol-6 (2H) –ylidene) methyl)-N, N-dimethylaniline*

Yellow powder.

FT-IR (KBr, ν_{max}/cm^{-1}): 3406 (=NH), 1596 (C=N), 1477 (C=C).

^{1}H NMR (CDCl$_3$, 300 MHz, 25 °C): 7.22-6.51 (m, 13H), 6.24 (s, 1H, =CH), 3.1 (d, 1H), 2.82; 2.86 (s, 12 H, 4N-CH$_3$) 2.31 (m, 1H), 1.78 -1.20 (m, 4H).

MS (ESI$^+$) m/z: 437(M+1)$^+$

Elemental analysis found (Calc.) for C$_{29}$H$_{32}$N$_4$: C, 79.78 (79.80); H, 7.39 (7.41); N, 12.83 (12.80).
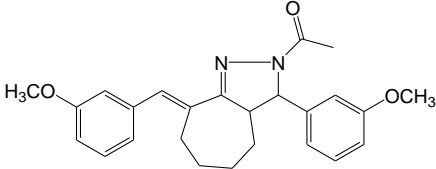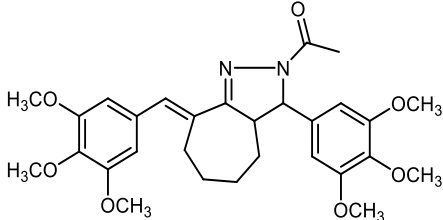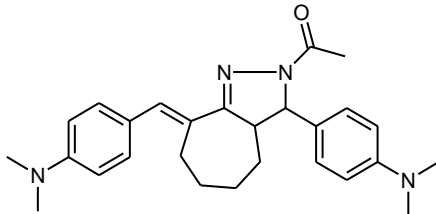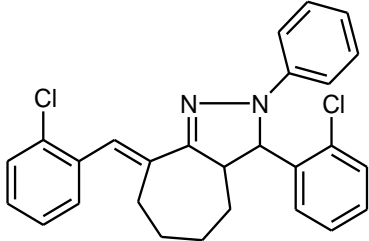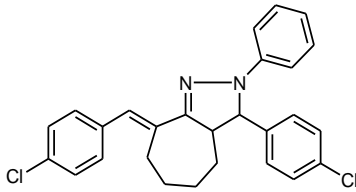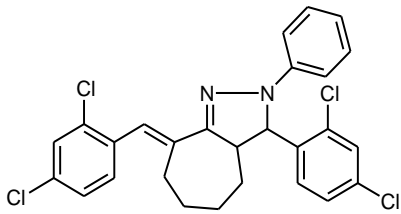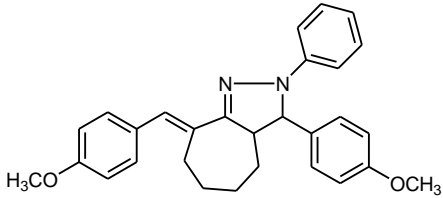
6.1.3. Synthesis and characterization of cycloheptanones analogues of curcumin (C1-C14)
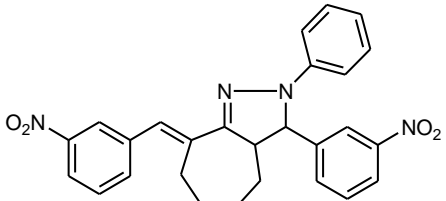
These were prepared in two steps. In first step, respective dibenzylidiene cycloheptanones were synthesized. A mixture of ethanol (20 ml) and sodium hydroxide solution (10%, 10 ml) was taken in a beaker and was maintained at temperature between 15 to 25ºC. The solution was vigorously stirred and one half of previously prepared mixture of appropriate aromatic aldehyde and cycloheptanone (in molar ratio of 2: 1) was added to it. After 20 min, the remaining aromatic aldehyde- cycloheptanones mixture was added. The reaction mixture was further stirred for 50 minutes. The solid was filtered off, washed with distilled water, and subjected to further purification by crystallization with ethyl alcohol.

In second step, synthesized substituted dibenzylidene cycloheptanones (1.2 mmol) from first step was dissolved in glacial acetic acid (5 ml), and hydrazine hydrate (1.5 mmol) was added to the solution. The solution was refluxed for 20 hours and monitored by TLC. The solvent was removed in vacuum and the residue was crystallized with ethyl alcohol. The remaining analogues were also prepared by the same procedure.

Table 6.3. Physical properties of cycloheptanone analogues of curcumin

Code	Structure	Solubility	Melting point (ºC)	Percentae yield (%)	Rf value
C1		Chloroform	140-142	75.00	0.47
C2		Chloroform	150-152	87.00	0.57
C3		Chloroform	173-174	71.00	0.48
C4		Chloroform	144-146	60.00	0.51
C5		Chloroform	160-162	75.00	0.55
C6		Chloroform	134-136	71.00	0.45

C7		Chloroform	220-222	56.0	0. 53
C8		Chloroform	156-158	63.00	0.59
C9		Chloroform	176-178	87.00	0.53
C10		Chloroform	180-182	73.00	0.55
C11		Chloroform	178-180	54.00	0.51
C12		Chloroform	144-146	68.00	0.63
C13		Chloroform	170-172	83.00	0.52

| C14 | | Chloroform | 134-136 | 65.00 | 0.51 |

Spectral data for cycloheptanone analogues of curcumin

Compound C1: *(E)-1-(8-benzylidene-3-phenyl-3a,4,5,6,7,8-hexahydro cycloheptac]pyrazol-2(3H)-yl)ethanone*

Yellow powder.

^{1}H NMR (CDCl$_3$, 300 MHz, 25 °C): 7.21-7.65 (m, 10H), 6.31 (s, 1H, =CH), 4.72 (d, 1H), 2.77 (m, 1H), 2.22 (s, 3H, CH$_3$), 1.31-1.95 (m, 8H).

MS (ESI$^+$) m/z: 345(M+1)$^+$

Elemental analysis Calc. (found) for C$_{23}$H$_{24}$N$_2$O: C, 80.20 (79.6); H, 7.84 (7.81); N, 8.38 (8.40).

Compound C2: *(E)-1-(8-(2-chlorobenzylidene)-3-(2-chlorophenyl)-3a,4,5,6,7,8-hexahydrocyclohepta[c]pyrazol-2(3H)-yl)ethanone*

Yellow powder.

^{1}H NMR (CDCl$_3$, 300 MHz, 25 °C): 7.11-7.85 (m, 8H), 6.51 (s, 1H, =CH), 4.75 (d, 1H), 2.75 (m, 1H), 2.25 (s, 3H, CH$_3$), 1.30-1.94 (m, 8H).

MS (ESI$^+$) m/z: 414(M+1)$^+$

Elemental analysis Calc. (found) for C$_{23}$H$_{22}$Cl$_2$N$_2$O: C, 66.83 (66.43); H, 5.36 (5.39); N, 6.78 (6.72).

Compound C3: *(E)-1-(8-(4-bromobenzylidene)-3-(4-bromophenyl)-3a,4,5,6,7,8-hexahydrocyclohepta[c]pyrazol-2(3H)-yl)ethanone*

Yellow powder.

^{1}H NMR (CDCl$_3$, 300 MHz, 25 °C): 7.12-7.70 (m, 8H), 6.40 (s, 1H, =CH), 4.63(d, 1H), 2.63 (m, 1H), 2.25 (s, 3H, CH$_3$), 1.30-1.95 (m, 8H).

MS (ESI$^+$) m/z: 504(M+2)$^+$

Elemental analysis Calc. (found) for C$_{23}$H$_{22}$Br$_2$N$_2$O: C, 55.00 (55.09); H, 4.42(4.40); N, 5.58 (5.53);

Compound C4: *(E)-1-(8-(2-hydroxybenzylidene)-3-(2-hydroxyphenyl)-3a,4,5,6,7,8-hexahydrocyclohepta[c]pyrazol-2(3H)-yl)ethanone*

Yellow powder.

^{1}H NMR (CDCl$_3$, 300 MHz, 25 °C): 7.11-7.78 (m, 8H), 6.30 (s, 1H, =CH),5.35 (s, 2H), 4.73(d, 1H), 2.53 (m, 1H), 2.27 (s, 3H, CH$_3$), 1.32-1.97 (m, 8H).

MS (ESI$^+$) m/z: 377(M+1)$^+$

Elemental analysis Calc. (found) for C$_{23}$H$_{24}$N$_2$O$_3$: C, 73.38 (73.45); H, 6.43 (6.46); N, 7.44 (7.47).

Compound C5: *(E)-8-(2,4-dichlorobenzylidene)-3-(2,4-dichlorophenyl)-3a,4,5,6,7,8-hexahydrocyclohepta[c]pyrazole-2(3H)-carbaldehyde*

Yellow powder.

^{1}H NMR (CDCl$_3$, 300 MHz, 25 °C): 7.08-7.68 (m, 6H), 6.20 (s, 1H, =CH), 4.53(d, 1H), 2.43 (m, 1H), 2.17 (s, 3H, CH$_3$), 1.22-1.77 (m, 8H).

MS (ESI$^+$) m/z: 483(M+1)$^+$

Elemental analysis Calc. (found) for C$_{23}$H$_{20}$Cl$_4$N$_2$O: C,57.29 (56.91); H, 4.18 (4.17); N, 5.81(5.78).

Compound C6: *(E)-1-(8-(2,4-dichlorobenzylidene)-3-(2,4-dichlorophenyl)-3a,4,5,6,7,8-hexahydrocyclohepta[c]pyrazol-2(3H)-yl)ethanone*

Yellow powder.

^{1}H NMR (CDCl$_3$, 300 MHz, 25 °C): 7.02-7.48 (m, 8H), 6.10 (s, 1H, =CH), 4.23(d, 1H), 2.23 (m, 1H), 2.07 (s, 3H, CH$_3$), 1.12-1.87 (m, 8H).

MS (ESI$^+$) m/z: 435(M+1)$^+$

Elemental analysis Calc. (found) for C$_{23}$H$_{22}$N$_4$O$_5$: C, 63.59 (63.68); H, 5.10 (5.14); N, 12.90 (12.93).

Compound C7: *(E)-1-(8-(3-methoxybenzylidene)-3-(3-methoxyphenyl)-3a,4,5,6,7,8-hexahydrocyclohepta[c]pyrazol-2(3H)-yl)ethanone*

Yellow powder.

^{1}H NMR (CDCl$_3$, 300 MHz, 25 °C): 7.02-7.48 (m, 8H), 6.10 (s, 1H, =CH), 4.23(d, 1H), 2.23 (m, 1H), 2.07 (s, 3H, CH$_3$), 1.12-1.87 (m, 8H), 3.68; 3.71 (s, 6H, 2OCH$_3$).

MS (ESI$^+$) m/z: 405(M+1)$^+$

Elemental analysis Calc. (found) for C$_{25}$H$_{28}$N$_2$O$_3$: C, 74.23 (74.72); H, 6.98 (6.97) ; N, 6.93 (6.91) .

Compound C8: *(E)-1-(8-(3,4,5-trimethoxybenzylidene)-3-(3,4,5-trimethoxyphenyl)-3a,4,5,6,7,8-hexahydrocyclohepta[c]pyrazol-2(3H)-yl)ethanone*

Yellow powder.

^{1}H NMR (CDCl$_3$, 300 MHz, 25 °C): 7.15-7.87 (m, 4H), 6.05 (s, 1H, =CH), 4.03(d, 1H), 2.01 (m, 1H), 2.05 (s, 3H, CH$_3$), 1.05-1.76 (m, 8H), 3.66; 3.73; 3.72 (s, 18H, 6OCH$_3$).

MS (ESI$^+$) m/z: 525(M+1)$^+$

Elemental analysis Calc. (found) for C$_{29}$H$_{36}$N$_2$O$_7$: C, 66.39 (66.23); H, 6.92 (6.93); N, 5.34 (5.37).

Compound C9: *(E)-1-(8-(4-(dimethylamino)benzylidene)-3-(4-(dimethylamino)phenyl)-3a,4,5,6,7,8-hexahydrocyclohepta[c]pyrazol-2(3H)-yl)ethanone*

Yellow powder.

^{1}H NMR (CDCl$_3$, 300 MHz, 25 °C): 7.10-7.77 (m, 8H), 6.15 (s, 1H, =CH), 4.21(d, 1H), 2.7 (m, 1H), 2.04 (s, 3H, CH$_3$), 1.12-1.85 (m, 8H), 3.75(s, 12H).

MS (ESI$^+$) m/z: 431(M+1)$^+$

Elemental analysis Calc. (found) for C$_{27}$H$_{34}$N$_2$O: C, 75.31 (75.44); H, 7.96 (7.93); N, 13.01 (12.98).

Compound C10: *(E)-8-(2-chlorobenzylidene)-3-(2-chlorophenyl)-2-phenyl-2,3,3a,4,5,6,7,8-octahydrocyclohepta[c]pyrazole*

Yellow powder.

^{1}H NMR (CDCl$_3$, 300 MHz, 25 °C): 7.15-7.67 (m, 13H), 6.25 (s, 1H, =CH), 4.25(d, 1H), 2.5 (m, 1H), 1.22-1.75 (m, 8H).

MS (ESI$^+$) m/z: 448(M+1)$^+$

Elemental analysis Calc. (found) for C$_{27}$H$_{24}$Cl$_2$N$_2$: C, 72.48 (72.41); H, 5.41 (5.44); N, 6.26 (6.29).

Compound C11*: (E)-8-(4-chlorobenzylidene)-3-(4-chlorophenyl)-2-phenyl-2,3,3a,4,5,6,7,8-octahydrocyclohepta[c]pyrazole*

Yellow powder.

^{1}H NMR (CDCl$_3$, 300 MHz, 25 °C): 7.12-7.69 (m, 13H), 6.35 (s, 1H, =CH), 4.20(d, 1H), 2.1 (m, 1H), 1.12-1.85 (m, 8H).

MS (ESI$^+$) m/z: 448(M+1)$^+$

Elemental analysis Calc. (found) for C$_{27}$H$_{24}$Cl$_2$N$_2$: C, 72.48 (72.09); H, 5.41 (5.42); N, 6.26(6.21).

Compound C12: *(E)-8-(2,4-dichlorobenzylidene)-3-(2,4-dichlorophenyl)-2-phenyl-2,3,3a,4,5,6,7,8-octahydrocyclohepta[c]pyrazole*

Yellow powder.

^{1}H NMR (CDCl$_3$, 300 MHz, 25 °C): 7.02-7.59 (m, 11H), 6.25 (s, 1H, =CH), 4.10(d, 1H), 2.8 (m, 1H), 1.02-1.95 (m, 8H).

MS (ESI$^+$) m/z: 517(M+1)$^+$

Elemental analysis Calc. (found) for C$_{27}$H$_{22}$Cl$_4$N$_2$:C, 62.81(62.47); H, 4.30 (4.26); N, 5.43 (5.42).

Compound C13: *(E)-8-(4-methoxybenzylidene)-3-(4-methoxyphenyl)-2-phenyl-2,3,3a,4,5,6,7,8-octahydrocyclohepta[c]pyrazole*

Yellow powder.

^{1}H NMR (CDCl$_3$, 300 MHz, 25 °C): 7.13-7.89 (m, 13H), 6.55 (s, 1H, =CH), 4.10(d, 1H), 2.76 (m, 1H), 1.08-1.94 (m, 8H), 3.65, 3.70(s, 6H,2 OCH$_3$).

MS (ESI$^+$) m/z: 439(M+1)$^+$

Elemental analysis Calc. (found) for C$_{29}$H$_{30}$N$_2$O$_2$:C,79.42 (79.19); H,6.89(6.83); N, 6.39 (6.37).

Compound C14: *(E)-8-(3-nitrobenzylidene)-3-(3-nitrophenyl)-2-phenyl-2,3,3a,4,5,6,7,8-octahydrocyclohepta[c]pyrazole*

Yellow powder.

^{1}H NMR (CDCl$_3$, 300 MHz, 25 °C): 7.23-7.79 (m, 13H), 6.45 (s, 1H, =CH), 4.20(d, 1H), 2.70 (m, 1H), 1.05-1.84 (m, 8H).

MS (ESI$^+$) m/z: 469(M+1)$^+$

Elemental analysis Calc. (found) for C$_{27}$H$_{24}$N$_4$O$_4$:C, 69.22 (69.02); H, 5.16 (5.17); N, 11.96 (11.93).

6.2. *In-vitro* Antimicrobial screening of curcumin analogues

6.2.1.*In-vitro* Antimicrobial screening of hexahydroindazole analogues of curcumin

The results of antimicrobial screening revealed that among the compounds screened A2, A3, B1 and B2 showed moderate antibacterial activity while compound A7 & A8 displayed good antibacterial activity when compared with standard drug ciprofloxacin. Particularly, compound A7 which is carrying methoxy group on aryl ring appears to exhibit highest antibacterial activity (zone of inhibition up to 21 mm) against *E. coli* and *S. aureus.*
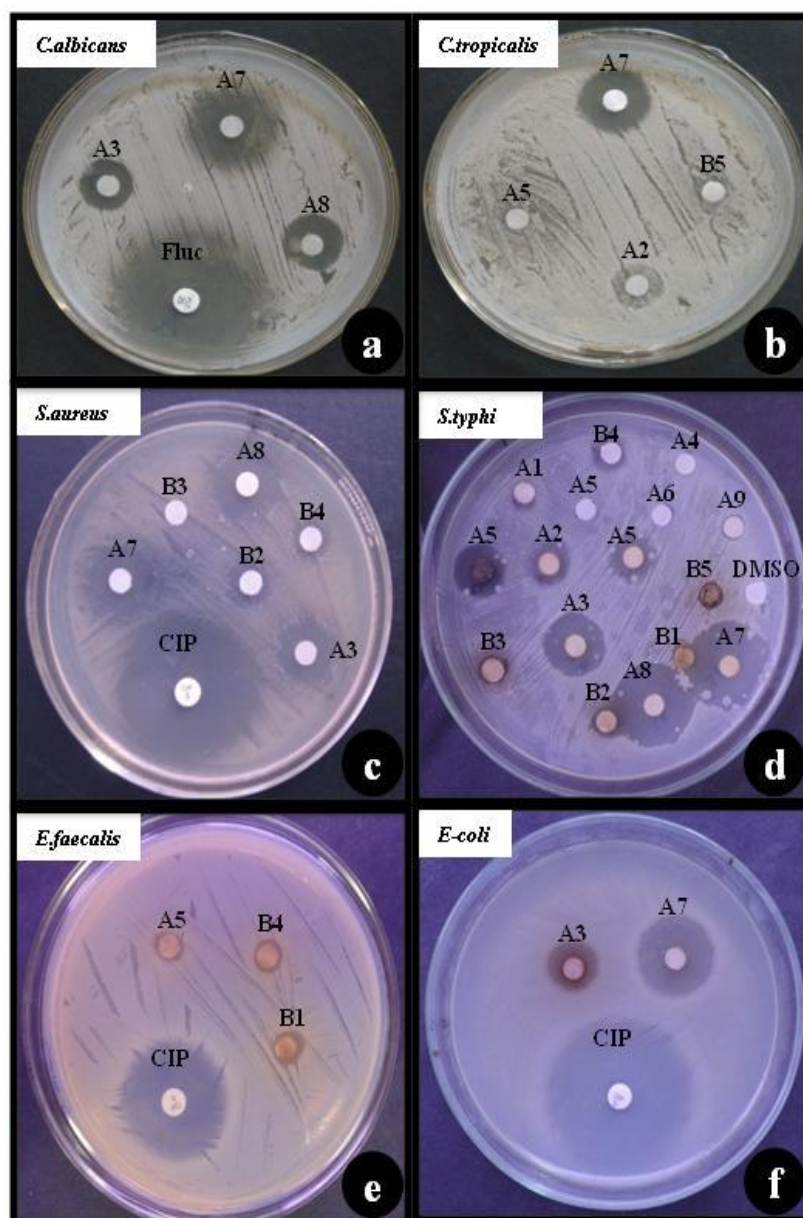
Figure 6.1. Antimicrobial activity of hexahydroindazole analogues of Curcumin **(a)** antifungal activity against *Candida albicans* with refrence to standard drug Fluconazole, A7 showing the strongest inhibition compare to A3 and A8 **(b)** antifungal activity against *C.tropicalis*, A7 showing clear zone of inhibition as compare to A5, B5 and A2 **(c)** Antibacterial against *S.aureus* with reference to standard drug Ciprofloxacin, A3, A8 and A7 showing inhibition much better than B3, B2,and B4 **(d)** antibacterial against *S.typhi*, A3, A5, A8, A7, A2, A5 and B4 showing inhibition zone **(e)** antibacterial against *E.faecalis* with reference to Ciprofloxacin as standard, A5, B4, and B1 showing less inhition compare to standard **(f)** antibacterial activity against *E-coli*, A7 and A3 showing good inhibition as compared to standard Ciprofloxacin.

Table6.4. Antimicrobial activity of hexahydroindazole analogues of curcumin

Comp code	Bacterial Strains Zone of inhibition (in mm)					Fungal Strains Zone of inhibition (in mm)		
	E.coli ATCC 35218	*S. typhi* MTCC 3216	*K.pneumoniae*	*S. aureus* ATCC 25323	*E. faecalis*	*C. albicans* ATCC 90028	*C. tropicalis* ATCC 750	*C. krusie*
A1	NA	NA	NA	10.37±0.38	9.70±0.36	NA	NA	NA
A2	15.60±0.26	14.37±0.12	14.87±0.15	13.20±0.17	15.83±0.19	14.80±0.25	12.53±0.18	12.83±0.15
A3	13.30±0.25	14.93±0.18	17.63±0.09	16.77±0.03	14.57±0.15	16.27±0.23	11.30±0.15	11.20±0.15
A4	9.40±0.12	NA	NA	11.73±0.38	10.50±0.21	13.37±0.09	NA	NA
A5	8.93±0.09	NA	10.27±0.09	11.70±0.12	NA	12.67±0.09	NA	NA
A6	8.07±0.09	NA	NA	10.23±0.15	9.03±0.12	NA	NA	NA
A7	21.43±0.18	17.20±0.17	20.40±0.11	22.53±0.09	20.33±0.15	23.0±0.12	21.50±0.12	19.77±0.15
A8	19.67±0.11	15.10±0.15	16.80±0.17	17.0±0.16	15.23±0.20	20.33±0.12	18.20±0.17	17.87±0.19
A9	10.90±0.06	NA	NA	10.03±0.18	12.10±0.20	11.93±0.09	NA	12.47±0.07
B1	13.93±0.09	NA	8.87±0.13	7.10±0.17	6.63±0.09	7.63±0.05	5.73±0.12	NA
B2	8.07±0.06	NA	NA	6.77±0.15	4.07±0.18	NA	NA	NA
B3	7.87±0.10	NA	NA	NA	NA	6.70±0.13	NA	5.93±0.09
B4	9.33±0.07	8.33±0.09	NA	5.57±0.12	4.87±0.09	NA	NA	NA
B5	8.90±0.08	NA	NA	NA	4.17±0.15	NA	NA	3.30±0.17
Cip	26.23±0.16	19.98±0.06	26.71±0.08	27.44±0.15	22.50±0.09	NA	NA	NA
Fluc	NA	NA	NA	NA	NA	25.33±0.05	24.65±0.05	24.06±0.04
DMSO	-	-	-	-	-	-	-	-

The value of each compound consisted of Mean ± SEM of 03 replicates.

Level of significance $p < 0.05$

Interestingly, triple substitution of methoxy group at *ortho, meta* and *para* position leads to a slight decrease in the potency (compound A8 zone of inhibition = 19.67mm). This may be due to the steric hindrance of these groups. It can be concluded that electron donating group (methoxy) significantly increases antibacterial activity. The derivatizationof B1 with chloro substitution on phenyl rings regained and enhanced the potency (Compound B1 zone of inhibition = 13.93mm) whereas methoxy (Compound B4 zone of inhibition = 9.33mm) and N,N-dimethylamino (B5, zone of inhibition = 8.90mm) substitutions exhibited moderate potency. However, Phenyl pyrazoline analogues (B1-B5) did not significantly increase the antibacterial potency.

The results of antifungal screening indicated that compounds, A2, A3, A4, A7 and A8 showed moderate to excellent antifungal activity. Compounds A2, A3 and A4 showed moderate activity against *C. albicans.* Interestingly, compound A3 also showed moderate activity against three fungal strains viz.*C. albicans, C. tropicalis, C. krusie.* Among the halogenated analogues chloro substitution at *ortho* or *para* position increased antifungal potency appreciably (compound A2 zone of inhibition = 14.80mm), (compound A4 zone of inhibition = 13.37mm) but chloro substitution at both *ortho* and *para* positions caused a marginal decrease in potency (compound A5 zone of inhibition = 12.67mm). This may be attributed to successful interactions of the compound with target protein(s) when chloro substitution is either at *ortho* or *para* postion. Out of 14 compounds, majority of the compounds showed considerable antimicrobial activity against tested strains.

6.2.2. *In vitro* antimicrobial study of pyrazole analogues of curcumin

The compounds were prepared by coupling substituted benzaldehydes with cyclopentanone in (molar ratio of 2:1) in a base catalyzed Claisen-Schmidt condensation followed by reaction with hydrazines (hydrazine hydrate, phenyl-hydrazine) and acetic acid. Antimicrobial activity of new pyrazole analogues of curcumin synthesized compounds are given in (Table 6.5).

The results of antibacterial screening revealed that among the screened compounds CP1, CP2 and CP8 showed moderate antibacterial activity. However, compounds CP10, CP11 and CP12 showed good antibacterial activity when compared with ciprofloxacin used as standard. Particularly, compound CP10 showed maximum antibacterial activity (Zone of inhibition up to 21mm) against *E. coli* and *S. aureus* (Figure 6.2). The substitution of chloro group at *ortho* and *para* positions led to slender decrease in potency (compound CP12 zone of inhibition =19mm).
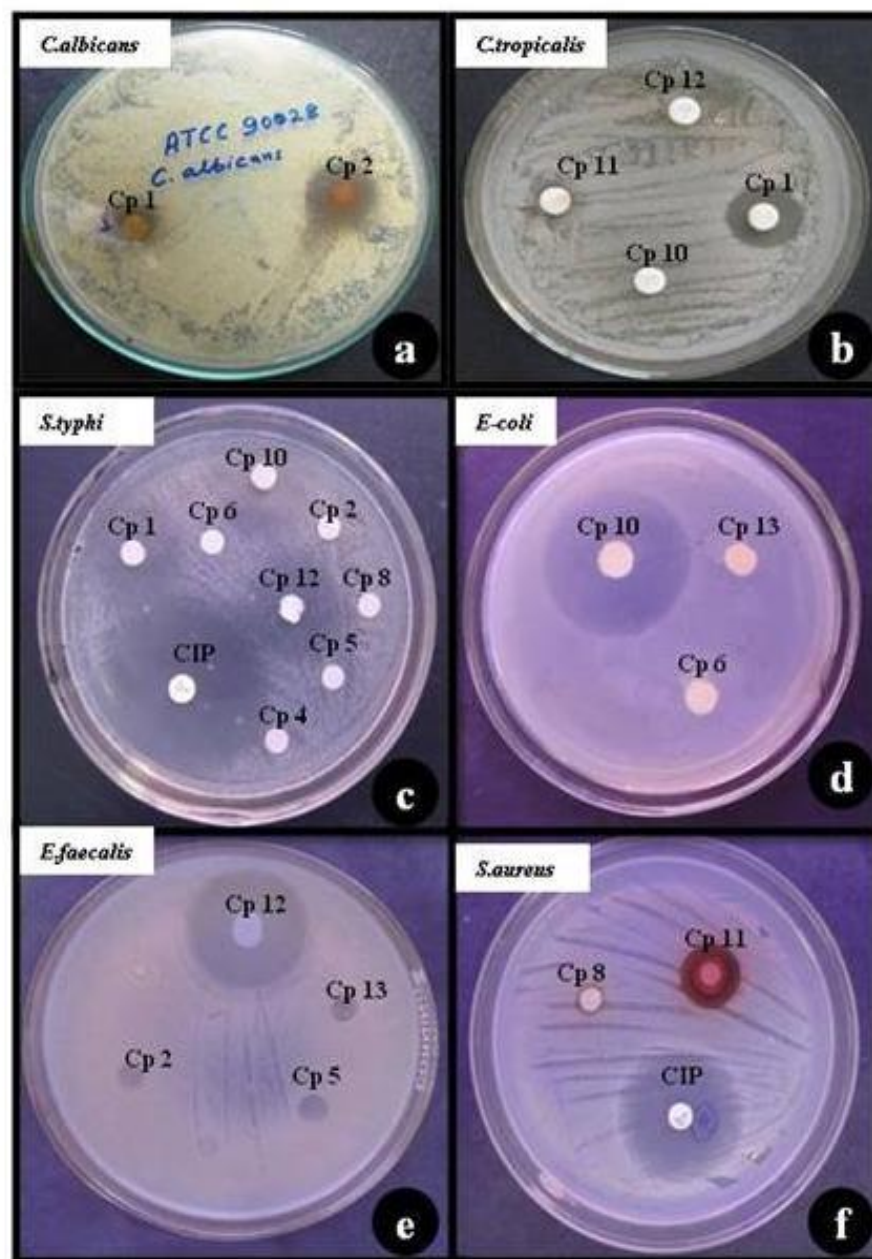
Figure 6.2 Bioassay plate showing antimicrobial effect of pyrazole analogues of Curcumin by agar well diffusion methods **(a)**CP1 &CP2 showing effective antifungal activity against *C. albicans* with reference to standard drug Fluconazole **(b)**CP1 showing effective inhibition zone against *C.tropicalis*, as compared to CP10, CP11, CP12 **(c)** Antibacterial activity against *S.typhi* with reference to standard drug Ciprofloxacin (CIP), CP1, CP10 and CP12 showing inhibition compared to CP2, CP4, CP5, CP6 and CP8 **(d)**CP10 showing excellent inhibition against *E. coli*, compared to CP6 and CP13 **(e)**CP12 showing effective antibacterial activity against *E.faecalis* compared to other analogues **(f)**CP11 showing inhibition zone against *S. aureus*, as compared to Ciprofloxacin.

Table 6.5. Antimicrobial activity of pyrazole analogues of curcumin.

Comp code	Microbial species							
	Bacterial Strains Zone of inhibition (in mm)					**Fungal Strains** Zone of inhibition (in mm)		
	E.coli ATCC 35281	*S.typhi* MTCC 3216	*P. aeruginosa* ATCC 27853	*S. aureus* ATCC 25323	*E.faecalis* (Clinical isolate)	*C. albicans* ATCC 90028	*C. tropicalis* ATCC 750	*C. krusie* ATCC 6258
CP1	12.73 ± 0.20	14.23 ± 0.70	10.66 ± 0.40	11.43 ± 0.90	-	8.73 ± 0.75	11.66 ± 0.17	-
CP2	10.45 ± 0.47	-	-	-	10.17 ± 0.47	11.49 ± 1.03	-	12.06 ± 0.15
CP3	12.35 ± 0.40	13.26 ± 0.15	12.06 ± 0.90	14.63 ± 0.85	12.26 ± 0.33	-	11.66 ± 0.47	10.70 ± 0.51
CP4	11.35 ± 1.07	-	-	11.30 ± 0.34		10.80 ± 0.51	10.30 ± 1.15	-
CP5	09.45 ± 1.15	-	9.60 ± 0.50	10.33 ± 0.61	11.26 ± 0.94	10.87 ± 0.80	-	09.24 ± 0.23
CP6	-	-	-	-	-	-	-	-
CP7	11.50 ± 0.37	-	13.60 ± 0.98	14.13 ± 0.21	-	12.65 ± 0.86		9.76 ± 0.45
CP8	13.40 ± 0.02	-	-	10.56 ± 0.45	-	10.15 ± 0.17	-	-
CP9	-	10.87 ± 0.79	10.53 ± 0.44	11.53 ± 0.25	-	-	10.13 ± 0.34	
CP10	21.50 ± 0.72	17.26 ± 0.15	15.76 ± 0.19	20.13 ± 0.22	14. 26 ±1.27	11.53 ± 0.32	-	10.51 ± 0.16
CP11	18.40 ± 1.10	-	17.33 ± 1.06	14.01 ± 0.15	-	13.86 ± 0.65	-	11.20 ± 0.86
CP12	19.64 ± 0.93	15.30 ± 0.91	16.06 ± 0.52	19.13 ± 1.65	15.40 ± 1.17	10.10 ± 0.53	-	10.53 ± 0.39
CP13		-	-	11.26 ± 0.25	10.90 ± 0.62	11.66 ± 0.40	-	16.13 ± 0.70
CP14	11.33 ± 0.35	10.53 ± 0.57	-	10.76 ± 0.56	-	09.16 ± 0.06	-	12.50 ± 0.66
Ciplo	28.06 ± 1.30	22.17 ± 0.45	29.76 ± 0.26	30.63 ± 0.49	26.40 ± 0.19	-	-	-
Fluco	-	-	-	-	-	21.35 ± 0.55	16.80 ± 0.15	20.93 ± 0.18
DMSO	-	-	-	-	-	-	-	-

The values of each compound consisted of Mean ± SEM of 03 replicates.

Level of significance $p < 0.05$.

The introduction of methoxy group at *meta* position in order to increase electron density resulted in diminished antibacterial activity (Compound CP7 zone of inhibition = 11mm). While substitution of methoxy group at *ortho*, *meta* and *para* position led to slight increase in potency (compound CP8 zone of inhibition=13 mm). This may be due to the favorable steric interaction of these groups. The results of antifungal screening indicated that compounds CP2, CP7, CP11, CP13 showed moderate to excellent antifungal activity. Compounds CP2, CP7 and CP11 showed moderate activity against *C. albicans*. Interestingly, compound CP13 showed good activity against two fungal strains viz. *C. albicans* and *C. krusie*. Methoxy substitution (compound CP13 zone of inhibition=16mm) increased antifungal potency significantly. Among the halogenated analogues chloro substitution at *para* position increased antifungal activity appreciably (compound CP11 zone of inhibition=13mm). The increase in potency of *para* substituted may be attributed to appropriate orientation of chloro to fit in binding site. However, majority of the compound synthesized showed substantial antimicrobial activity against tested strains.

6.2.3. *In vitro* anti microbial study of cycloheptanone analogues of curcumin

The compounds were prepared by coupling substituted benzaldehydes with cycloheptanone in (molar ratio of 2:1) in a base catalyzed Claisen-Schmidt condensation followed by reaction with hydrazines (hydrazine hydrate, phenyl-hydrazine) and acetic acid. Antimicrobial activity of synthesized cycloheptanone analogues of curcumin are given in (Table 6.6).

Table 6.6: Antimicrobial activity of cycloheptanone analogues of curcumin

Comp Code	Bacterial Strains Zone of inhibition (in mm)					Fungal Strains Zone of inhibition (in mm)		
	E.coli ATCC 35218	*S. typhi* MTCC 3216	*K. pneumonia*	*S. aureus* ATCC 25323	*E. faecalis*	*C. albicans* ATCC 90028	*C. tropicalis* ATCC 750	*C. krusie*
C1	13.32±0.13	12.76±0.21	14.82±0.08	NA	NA	14.23±0.32	12.62±0.21	13.78±0.23
C2	12.40±0.23	4.27±0.11	4.67±0.05	NA	12.43±0.13	NA	NA	NA
C3	15.30±0.21	11.93±0.08	7.23±0.05	NA	NA	10.21±0.13	NA	NA
C4	NA	12.23±0.06	NA	NA	12.70±0.11	15.27±0.07	11.31±0.32	NA
C5	8.73±0.06	16.12±0.10	10.25±0.03	10.20±0.22	NA	11.47±0.04	14.41±0.23	12.87±0.21
C6	NA	13.24±0.12	7.08±0.05	8.23±0.25	15.03±0.10	10.45±0.08	16.21±0.31	16.67±0.04
C7	11.43±0.15	15.10±0.07	10.40±0.11	12.33±0.10	10.23±0.11	13.0±0.02	NA	NA
C8	9.67±0.11	16.20±0.17	11.20±0.07	NA	5.73±0.80	10.33±0.14	NA	NA
C9	8.90±0.06	13.21±0.21	17.21±0.02	13.05±0.14	15.20±0.60	6.93±0.09	7.23±0.23	NA
C10	10.63±0.09	12.86±0.11	12.47±0.03	5.30±0.14	18.23±0.04	12.43±0.07	12.23±0.11	9.65±0.34
C11	8.17±0.06	15.16±0.26	9.56±0.08	17.07±0.05	14.03±0.08	NA	10.32±0.32	7.76±0.35
C12	6.57±0.10	11.53±0.02	7.87±0.12	NA	15.34±0.05	12.60±0.11	13.56±0.76	4.67±0.07
C13	12.33±0.05	7.23±0.09	14.76±0.21	NA	NA	15.81±0.21	12.76±0.21	NA
C14	7.90±0.09	10.22±0.05	13.65±0.05	NA	NA	14.21±0.32	12.38±0.12	12.30±0.11
Cip	26.23±0.16	19.98±0.06	26.71±0.08	27.44±0.15	22.50±0.09	16.21±0.22	NA	NA
Fluc	NA	NA	NA	NA	NA	25.33±0.05	24.65±0.05	24.06±0.04
DMSO	-	-	-	-	-	-	-	-

The values of each compound consisted of Mean ± SEM of 03 replicates.
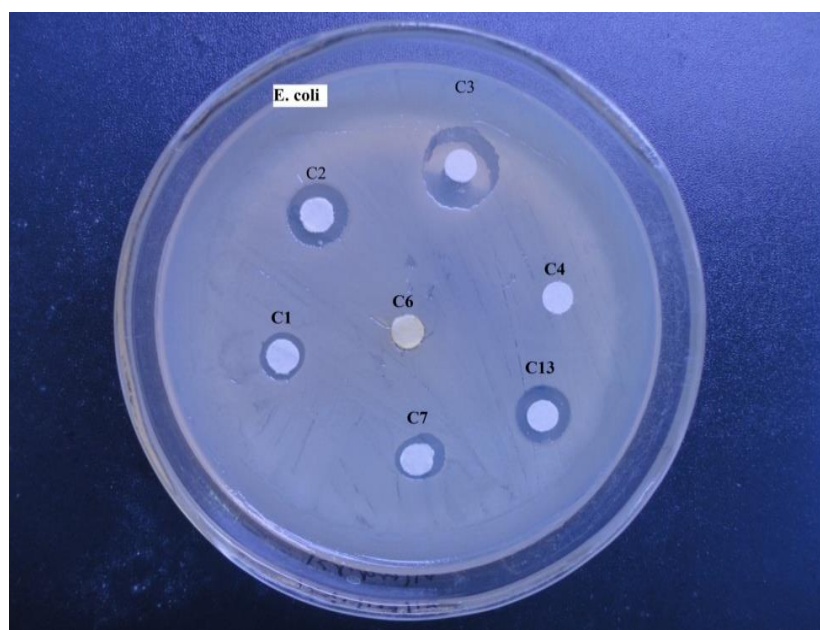
Level of significance $p < 0.05$.

Figure:6.3 Bioassay plate showing antimicrobial effect of cycloheptanone analogues of Curcumin by agar disc diffusion methods

The results of antibacterial screening revealed that among the screened compounds C1, C2 and C3 showed good antibacterial activity when compared with ciprofloxacin used as standard. Particularly, compound C3 showed maximum antibacterial activity (Zone of inhibition up to 15mm) against *E.coli* and *S. aureus* (Figure 6.3). Rest of the compounds except C10 and C13 did not show optimum activity (Zone of inhibition up to 10mm-12mm) against *E. coli*.

Compounds C10 showed good activity against *C. albicans*. Rest of the compounds showed moderate activity against two fungal strains viz. *C. albicans* and *C. krusie*. The decrease in antibacterial and antifungal activity of this series of compounds may be attributed to increase in bulkiness of ring (cycloheptanone) although it is infantile to conclude on their structure activity relationship (SAR) and it needs further to be expored and investigated.

6.3. Antimalarial screening of curcumin analogues

The synthesized compounds were screened for *in vitro* antimalarial activity against CQ - resistant (W2 clone) of *Plasmodium falciparum* using [³H] hypoxanthine incorporation assay. IC$_{50}$values were calculated from nonlinear regression analysis using *"dose-response curve"* plotted between effective concentration and *Plasmodium* viability (Fig 6.4). The results were evaluated with the software Origin 8.0 for determination of the dose-response curves plotted with sigmoid fit.
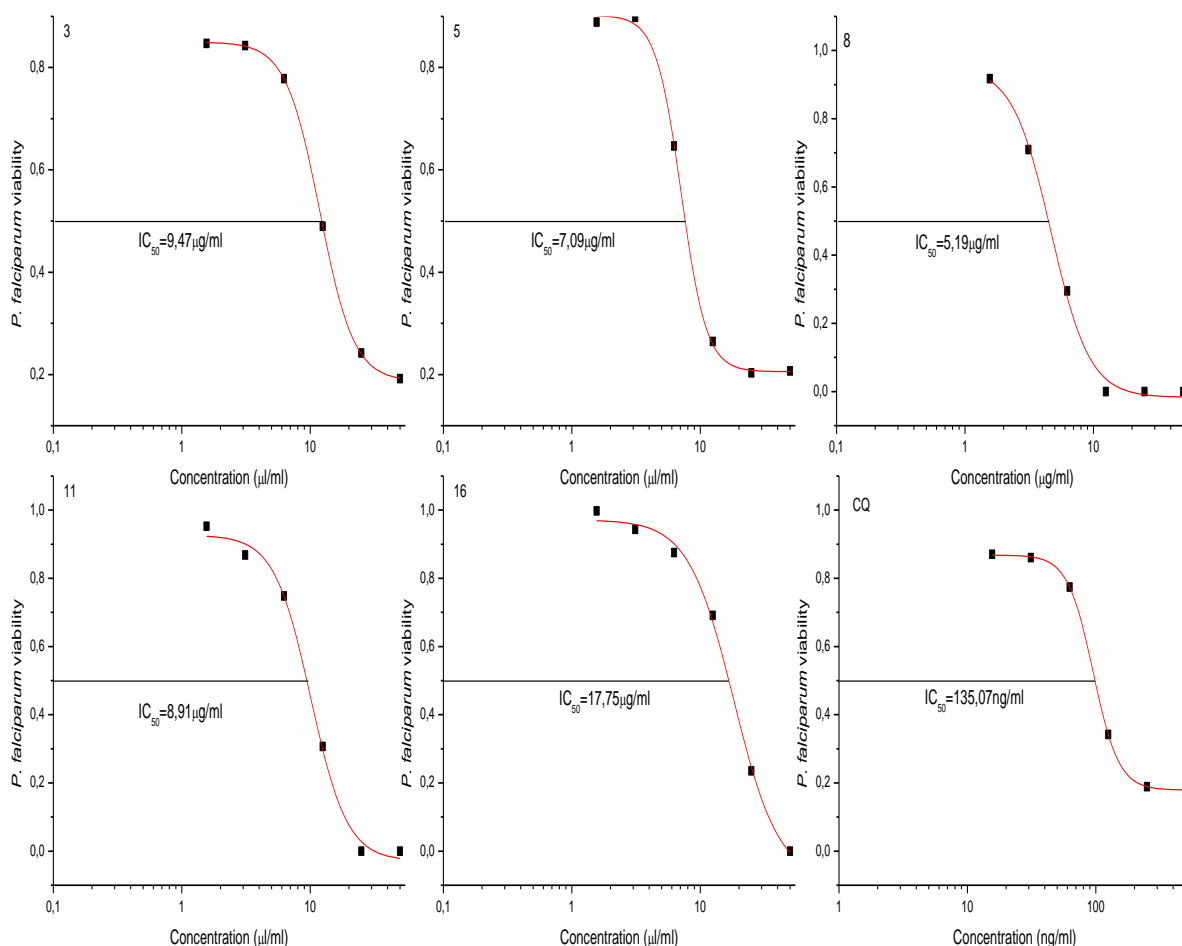
Figure 6.4 - Dose-response curves of the samples (A3, A5, A8, B2, CP2) tested against *P. falciparum* (W2 strain) showing the values of inhibitory concentration of 50% growth of parasite (IC$_{50}$)

Table 6.7. Inhibitory concentrations (IC$_{50}$) of active samples tested against *P. falciparum* clone W2 (Chloroquine-resistant).

Comp code	IC$_{50}$ (µg/ml) against *P. falciparum* (W2 strain) Mean± SD	Classification
A1	>50	Inactive
A2	25<IC$_{50}$<50	Weakly active
A3	9.47±2.59	Active
A4	>50	Inactive
A5	7.09±2.69	Active
A6	>50	Inactive
A7	>50	Inactive

A8	5.19 ± 1.12	Active
A9	>50	Inactive
B1	$25 < IC_{50} < 50$	Weakly active
B2	8.91 ± 0.39	Active
B3	>50	Inactive
B4	>50	Inactive
B5	>50	Inactive
CP1	$25 < IC_{50} < 50$	Weakly active
CP2	17.75 ± 2.08	Moderately active
CP3	$25 < IC_{50} < 50$	Weakly active
CP4	>50	Inactive
CP5	>50	Inactive
CP6	>50	Inactive
CP7	$25 < IC_{50} < 50$	Weakly active
CP8	>50	Inactive
CP9	>50	Inactive
CP10	>50	Inactive
CP11	>50	Inactive
CP12	>50	Inactive
CP13	$25 < IC_{50} < 50$	Weakly active
CP14	>50	Inactive
C1	>50	Inactive
C2	>50	Inactive
C3	>50	Inactive
C4	>50	Inactive
C5	>50	Inactive
C6	$25 < IC_{50} < 50$	Weakly active
C7	>50	Inactive
C8	>50	Inactive
C9	>50	Inactive
C10	$25 < IC_{50} < 50$	Weakly active
C11	>50	Inactive
C12	>50	Inactive
C13	>50	Inactive
C14	>50	Inactive

The samples were classified according to the following criteria:

- ✓ **Very active –** IC_{50} value lower than 1µg/ml;
- ✓ **Active -** IC_{50} value 1 - 15µg/ml;
- ✓ **Moderately active -** IC_{50} value 15.1 - 25 µg/ml,
- ✓ **Weakly active –** IC_{50} value 25.1 - 50 µg/ml,
- ✓ **Inactive -** IC_{50} value higher than 50 µg/ml.

Samples A3, A5, A8 and B2 were active. Sample CP2 was moderately active and sample CP3was weakly active. The remaining samples were inactive. The antimalarial drug Chloroquine was used as standard drug and is considered very active with IC_{50}=0.135µg/ml. The results have been summarized in table 6.8.

Table 6.8. Antimalarial activity classification of samples tested against *P. falciparum* clone W2 (Chloroquine-resistant)

Sample code	IC_{50} (µg/ml) Mean ± SD	Classification
A3	9.47±0.71	Active
A5	7.09±0.69	Active
A8	5.19±0.32	Active
B2	8.91±0.39	Active
CP2	17.75±0.98	Moderately active
Chloroquine	0.135±0.011	Very active

The values of each compound consisted of Mean ± SD of 03 replicates.

6.3.1. Cytotoxicity study of curcumin analogues active against HepG2 line cells

The cytotoxicity assay was performed as described by Moss and colaborators (1983) with modificatons. HepG2 line cells were used for the tests. The results were evaluated with the software Origin 8.0 for determination of the dose-response curves plotted with sigmoidal fit.

The 50% cytotoxic concentration of cells (CC_{50}) was determined by comparison with controls without drugs and standard drug (Chloroquine). The selectivity index (SI) was calculated based on ratio of CC_{50} and IC_{50} values. The samples 3 and 16 were cytotoxic. The others samples were considered safe.

Table 6.9. Cytotoxic concentrations (CC_{50}) of selected curcumin analogues that inhibits growth of 50% of HepG2 cells.

Comp code	CC_{50} (µg/ml)
A3	77.18 ± 1.21
A5	472.02 ± 6.04
A8	78.31 ± 4.09
B2	333.48 ± 17.54
CP2	104.22 ± 9.63
Chloroquine	191.49 ± 6.43

The values of each compound consisted of Mean $\pm$ SD of 03 replicates.

6.3.2 Comparison of anti-malarial activity and cytotoxicity on basis of selectivity index

The results of antimalarial screening revealed that among the compounds screened A3, A5, A8 & B2 displayed significant antimalarial activity. Among the halogenated analogues (A3-A5) the chloro analogues (A3 IC_{50}=9.47µg/ml, A5 IC_{50}=7.09 µg/ml) were the active ones. This is in accordance with presence of chloro group in diverse active antimalarial molecules including Chloroquine, Pyronalidine and others [Manohar *et al.* 2010]. It is noticed that mono substitution either at *ortho* or *para* position increased the antimalarial potency conspicuously (IC_{50}=9.47µg/ml) with respect to unsubstituted. While chloro substitution at both *ortho* and *para* position caused atrivial augment in potency. (A5, IC_{50} =7.09 µg/ml). The addition of methoxy group in an endeavor to increase electron density has decreased the potency of unsubstituted analogues (IC_{50}=8.91 µg/ml) when the methoxy group is at *para* position. Trisubstituted methoxy group increased the potency A8 (IC_{50} =5.19µg/ml). In case of electron withdrawing (A6, Nitro, IC_{50}>50µg/ml) and electron releasing (A9, methylated amine, IC50>50µg/ml) substituent were found to be inactive. Among Phenyl pyrazoline analogues (B1-B5) *para* chloro substitution on phenyl rings retrieved and enhanced the potency (Compound B2 IC_{50}=8.91 µg/ml,) signifying that substitutions may result in restitution of potency. Whereas, methoxy (Compound B4 IC_{50}>50µg/ml) and N,Ndimethylamino (B5 IC_{50}>50µg/ml) substitutions exhibited low effectiveness. Phenyl pyrazoline analogues (B1-B5) did not significantly increase the antimalarial potency except *para* chloro substitution (B2). The most active compounds (IC_{50}<10 µg/ml i.e A3, A5, A8, A11and B2) were further evaluated for their cytotoxicity against HepG2 cell line.

Table 6.10 Comparison of anti-malarial activity and cytotoxicity on basis of selectivity index

Comp code	CC_{50} (µg/ml)	IC_{50} (µg/ml)	SI
3	77.18 ± 0.31	9.47 ± 0.21	8.15
5	472.02 ± 0.36	7.09 ± 0.16	66.57
8	78.31 ± 0.21	5.19 ± 0.29	15.09
11	333.48 ± 0.12	8.91 ± 0.30	37.43
16	104.22 ± 0.18	17.75 ± 0.16	5.87
Chloroquine	191.49 ± 0.23	0.135 ± 0.28	1418.44

CC_{50} = 50% Cytotoxic concentration

IC_{50}= 50% Inhibitory concentration

SI = selectivity index

All tested compounds except A3 were found to be devoid of cytotoxicity at inhibitory concentrations. This indicates their safety in the mammalian system. Additionally, these compounds were found to possess good selectivity index (SI=8-67) showing their selectivity towards malaria parasite. The selectivity index (SI) was calculated based on ratio of CC_{50} and IC_{50} values. The Cycloheptanone analogues (C1-C14) of curcumin did not show any promising antimalarial activity against *P. falciparum* clone W2 (Chloroquine-resistant). It might be due to presence of bulky group (cycloheptanone). These analogues need to be further explored for the treatment of malaria.

In summary, this study allows us to conclude that enviable improvement of antimalarial activity in hexahydroindazole analogues of curcumin requires (a) electron donating group (methoxy) at the *ortho*, *meta* and *para* positions, (b) electron withdrawing (chloro) group at the *ortho* and *para* postions. Although, it is infantile to arrive at the conclusion on detailed comprehensive structure activity aspect of these compounds and further assessment is desirable to use them for clinical study. Due to straightforward synthesis, these curcumin analogues embody a novel scaffold for developing new, affordable and effective antimalarial drugs with less chance of developing cross resistance.

6.4. *In silico* study of analogues of curcumin

In following section molecular docking study of analogues of curcumin is presented.

6.4.1. Molecular Docking study of hexahydroindazole analogues of curcumin

The combinatorial chemistry and virtual screening have rapidly increased in drug discovery. The need for minimizing extremely time-consuming steps of synthesis and

biological screening is important and thus they are good tools for predicting drug-likeness has also increased. The molecular descriptors have been employed to predict various human ADMET processes and other pharmacokinetic parameters such as oral absorption, bioavailability, skin penetration, clearance, volume of distribution, and metabolism [Clark 2003,Didziapetris *et al.*2003].

Predicting ADME properties at an early stage of drug discovery and development process is very important to remove compounds with poor pharmacokinetic properties and minimize extremely expensive and time-consuming steps. In the present study all the hexahydroindazole analogues of curcumin were predicted for different properties like drug-likeliness, Human intestinal absorption, *in vitro* skin permeability, *in vitro* plasma protein binding and water solubility in buffer system using PreADMET server. The results are summarized in Table 6.11.

Table 6.11. Theoretical ADME prediction of hexahydroindazole analogues of curcumin using PreADMET Server.

Comp code	LogP	Human intestinal Absorption (%)	*In vitro* skin permeability (logKp, cm/hour)	*In vitro* plasma protein binding (%)	Water solubility in buffer system mg/L
A1	4.62	99.54	-2.45	93.96	403.4
A2	5.70	99.68	-2.42	94.26	45.21
A3	3.61	94.30	-2.95	90.87	207.1
A4	5.98	99.68	-2.45	100	144.0
A5	7.01	99.59	-2.27	100	5.57
A6	3.69	93.90	-2.42	93.48	5.53
A7	4.69	97.37	-2.82	89.91	128.1
A8	4.10	98.91	-3.40	87.51	15.57
A9	4.82	98.31	-2.52	92.61	55.88
B1	8.23	100	-1.77	100	5.37×10^{-6}
B2	8.27	100	-1.76	100	1.50×10^{-5}
B3	8.85	100	-1.69	100	5.77×10^{-7}
B4	7.07	99.32	-2.05	96.34	3.77×10^{-5}
B5	7.10	100	-1.78	93.07	5.83×10^{-6}

Comparative docking of glucosamine-6-phosphate synthase (GlcN-6-P synthase) protein with the curcumin analogues and the standard drug Fucanozole and Amphotericin B, yielded best possible conformations with parameters including the binding energy, docked energy, inhibition constant and RMSD (Table 6.12). All the molecules showed very good binding and docking energy ranging from -5.40 Kcal/mol to -10.02 Kcal/mol and -4.86 to -10.96 Kcal/mol respectively (Figure 6.5). The minimum docked energy was

found in the analogue A7 (-10.96 kcal/mol) with an estimated inhibition constant of 4.50×10^{-8} and RMSD 0.56Å. Whereas, docked energy of the standard drugs Fluconazole was -5.67 kcal/mol with an inhibition constant of 5.53×10^{-5} and RMSD 1.97Å. The accuracy of docking study was evaluated by the root-mean square deviation (RMSD) of docked ligand from original crystal structure. RMSD less than 1.0 Å was considered as excellent.

Table 6.12. Molecular docking of hexahydroindazole analogues of curcumin with glucosamine-6-phosphate synthase.

Comp code	Binding Energy (Kcal/mol)	Docking Energy (Kcal/mol)	Inhibition constant (M)	Amino acid residue involved in H-bond	Bond Length (Å)	RMSD (Å)
A1	-9.25	-10.03	1.67×10^{-7}	Arg 73:HH1::Dp1:NA His 77:HE2::Dp1:NA	1.67 2.18	0.81
A2	-9.99	-10.78	4.79×10^{-8}	Arg 73:HE::Dp2:OA Arg 73:HH4::Dp2:NA	2.05 2.08	0.92
A3	-9.57	-10.28	9.63×10^{-8}	Gly 99:HN::Dp3:OA	1.90	0.99
A4	-8.19	-8.54	9.97×10^{-7}	No H- Bonds	--	1.12
A5	-9.56	-9.64	9.80×10^{-8}	No H- Bonds	--	1.20
A6	--	--	--	--	--	
A7	-10.02	-10.96	4.50×10^{-8}	Gly 99:HN::Dp7:OA	2.00	0.56
A8	-6.93	-8.48	8.57×10^{-6}	Arg 73:HH21::Dp8:OA His 77:HE2::Dp8:OA	1.68 2.13	1.02
A9	-5.40	-4.86	1.10×10^{-4}	His 71:HE2::Dp9:NB	1.88	1.11
B1	-7.64	-8.35	2.49×10^{-6}	His 77:HE2::Dp10:NA	2.01	0.96
B2	-7.51	-8.40	3.14×10^{-6}	No H- Bonds	--	1.23
B3	-8.69	-9.07	4.29×10^{-7}	No H- Bonds	--	1.20
B4	-8.53	-8.40	5.59×10^{-7}	Cys 1:SG::Dp13:OA	2.93	0.95
B5	-7.12	-7.55	6.05×10^{-6}	No H- Bonds	--	1.23
Flucanozole	-5.81	-5.36	5.53×10^{-5}	Arg 73:HH21::DF:OA Arg 73:HE::DF:OA His 77:HE2::Dp10:NA	2.20 2.09 1.87	1.97

A significant number of drugs and drug candidates in clinical development are halogenated structures. The formation of halogen bonds in ligand-target complexes is recognized as a kind of intermolecular interaction that favorably contributes to the stability

of protein-ligand complexes. The insertion of halogen atoms has been used in innumerous cases of hit-to-lead or lead-to-drug conversions [Buchini *et al.*2008, Bonnefous *et al.* 2009, Leite *et al.* 2007].
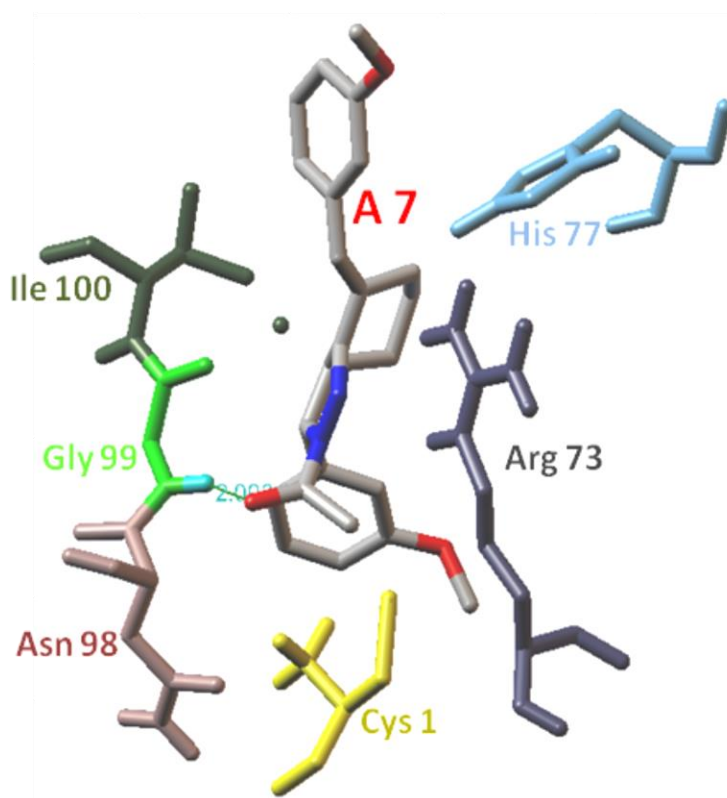

Figure 6.5. Interaction of compound A7 with GlcN-6-P

The incorporation of halogen atoms increases membrane permeability, improves the oral absorption and skin penetration etc.[Buchini *et al.* 2008]. It is generally accepted that halogen atoms are not capable of significant hydrogen bonding. Six analogues containing chlorine atom (A2, A4, A5, B2, B3 and B5) did not form any hydrogen bond with the amino acids of GlcN-6-P synthase, but showed very good binding and docking energy, since the halogens are endowed with the ability to establish intermolecular bonds in a fashion that resembles the H-bonds.

The molecular docking results of compound A7 showed very good binding energy and RMSD, even in *in vitro* studies also A7 emerged as active against all tested microorganisms, so it can be inferred that the activity may be due to inhibition of enzyme GlcN-6-Psynthase. The enzyme catalyses a complex reaction involving ammonia transfer from L-glutamine to Fru-6-P followed by isomerisation of the formed fructosamine-6-phosphate to glucosamine-6-phosphate.

6.4.2 Molecular Docking study of pyrazole analogues of curcumin

A significant bottleneck in the drug discovery procedures, especially in the later stages of lead discovery, is analysis of the ADME and overt toxicity properties of drug candidates. Nearly half of all drugs fail in clinical trials because of poor ADME and toxicity properties. Consequently, there is increasing interest in the early prediction of ADME properties, the objective of escalating the success rate of compounds reaching development [Leite *et al.* 2007]. Predicting ADME properties at an initial stage of drug discovery and development process is imperative to discard problematic candidates to reduce the amount of wasted time and resource, and streamline the overall development process.

In the present study, pyrazole analogues of curcumin were predicted for different properties like Log P, Human intestinal absorption, *in vitro* skin permeability, *in vitro* plasma protein binding and *in vivo* blood-brain barrier penetration using PreADMET server. The results are summarized in Table 6.13.

Table 6.13: Theoretical ADME prediction of pyrazole analogues of curcumin using PreADMET Server.

Comp Code	LogP	Human intestinal Absorption (%)	*In vitro* skin permeability (logKp, cm/hour)	*In vitro* plasma protein binding (%)	*In vivo* blood-brain barrier penetration
CP-1	4.07	99.52	-2.62	94.33	1.16
CP-2	5.39	99.67	-2.58	93.29	0.66
CP-3	3.30	94.13	-3.18	89.01	0.63
CP-4	5.41	99.67	-2.61	99.50	0.52
CP-5	5.80	99.61	-2.40	100	1.91
CP-6	4.16	92.93	-2.59	94.58	0.07
CP-7	4.06	97.37	-2.99	89.06	1.11
CP-8	3.61	99.06	-3.55	85.14	0.58
CP-9	4.41	98.27	-2.67	92.19	0.13
CP-10	6.42	100	-1.86	82.52	8.14
CP-11	6.79	100	-1.86	82.31	8.91
CP-12	7.69	100	-1.77	81.43	11.92
CP-13	5.92	99.31	-2.16	95.36	0.63
CP-14	6.07	100	-1.87	93.15	3.29

Molecular docking of two different active sites (Active site 1, amino acid series: Cys1, Arg73, Thr76, His77, Asn98, Gly99, Ile100 and active site 2, amino acid series: Gly301, Thr302, Ser303, Ser347, Gln348, Ser349, Thr352, Lys485, Ala602 and Val605) of

glucosamine-6-phosphate synthase (GlcN-6-P synthase) protein with the pyrazole analogues of curcumin and the standard drug Flucanozole yielded best possible conformations with parameters including the docked energy, inhibition constant and RMSD as presented in the table (Table 6.14 & 6.15).

Table 6.14. Molecular docking of pyrazole analogues of curcumin with glucosamine-6-phosphate synthase at Active Site1.

Comp code	Docking Energy (Kcal/mol)	Inhibition constant (M)	Amino acid residue involved in H-bond	Bond Length (Å)	RMSD (Å)
CP1	-9.77	2.16 x 10^{-7}	Thr76	2.17	1.05
			His77	1.84	
CP2	-9.34	4.08 x 10^{-7}	NB	NB	1.09
CP3	-10.22	6.87x 10^{-8}	Trp74	2.04	0.85
			Thr76	1.69	
			Gly99	1.73	
CP4	-9.14	7.70 x 10^{-7}	Thr76	1.97	1.10
CP5	-8.51	4.76 x 10^{-7}	His86	1.8	1.19
CP6	NA	NA	NA	NA	NA
CP7	-10.33	1.16 x 10^{-7}	His77	1.89	0.72
CP8	-9.51	3.35 x 10^{-7}	Gly99	2.13	1.01
CP9	-8.55	5.41 x 10^{-6}	Arg73	1.96	1.20
CP10	-10.85	1.08 x 10^{-7}	His77	1.90	0.82
CP11	-10.58	1.44 x 10^{-7}	His77	1.81	0.81
CP12	-11.12	5.23 x 10^{-8}	His77	1.91	0.74
CP13	-10.51	3.43 x 10^{-7}	His77	2.10	0.85
CP14	-9.74	1.61 x 10^{-6}	Arg73	1.89	1.00
			His104	2.11	
Flucanozole	-5.36	5.53x10^{-5}	Arg 73	2.20	1.34
			Arg 73	2.09	
			His 77	1.87	

Table 6.15: Molecular docking of pyrazole analogues of curcumin with glucosamine-6-phosphate synthase at Active Site 2.

S.No	Sample code	Docking Energy (Kcal/mol)	Inhibition constant (M)	Amino acid residue involved in H-bond	Bond Length (Å)	RMSD (Å)
1	CP1	-9.34	1.36×10^{-6}	Ala602	2.15	1.18
2	CP2	-9.67	3.3×10^{-7}	Gln348	1.95	1.11
				Ser349	2.22	
3	CP3	-9.80	2.80×10^{-7}	Gln348	1.81	1.08
				Ser349	1.90	
4	CP4	-10.57	3.0×10^{-7}	Gln348	2.07	0.86
				Ser349	2.12	
5	CP5	-9.48	4.12×10^{-7}	Gln348	2.10	1.16
				Ser349	2.16	
6	CP6	NA	NA	NA	NA	NA
7	CP7	-10.75	2.59×10^{-7}	Gln348	2.07	0.83
				Ala602	2.13	
8	CP8	-10.60	6.91×10^{-7}	Val605	1.83	0.85
9	CP9	-10.64	1.18×10^{-7}	Thr302	1.92	0.85
10	CP10	-12.18	1.44×10^{-8}	NB	NB	0.68
11	CP11	-12.32	8.31×10^{-9}	NB	NB	0.61
12	CP12	-11.35	5.35×10^{-8}	NB	NB	0.71
13	CP13	-10.51	1.03×10^{-6}	Gly301	2.04	0.86
14	CP14	-11.04	1.20×10^{-7}	NB	NB	0.73
15	Flucanozole	-6.57	4.7×10^{-5}	Gln348	2.35	1.28
				Ser349	2.02	

Comparative docking of GlcN-6-P synthase with the pyrazole analogues of curcumin and the standard drug flucanozole revealed that the docked energy for the compound CP10, CP11, CP12 was -10.85, -10.58, -11.12 kcal/mol at active site 1 and -12.18, -12.32, -11.35 kcal/mol at active site 2 with an estimated inhibition constant of 1.08×10^{-7}, 1.44×10^{-7}, 5.23×10^{-8} and 1.44×10^{-8}, 8.31×10^{-9}, 5.35×10^{-8} respectively (Figure 6.6). The docked energy of the Flucanozole was only -5.36 at active site 1 and -6.57 kcal/mol at active site 2

with an inhibition constant of 5.53×10^{-5} and 4.7×10^{-5} respectively. In the first active site the geometry of compounds CP10, CP11 and CP12 are "frozen" in the binding pocket due to strong and stable hydrogen bonds formed between the amido moiety of the inhibitor and the His77 amino acid residue present in the binding site and well conserved in GlcN-6-P synthase sequences from various organisms [Smith *et al.*1996]. Whereas, in the second active site there is no hydrogen bond formed with any of the three compounds but the docking energy and inhibition constant were minimum.
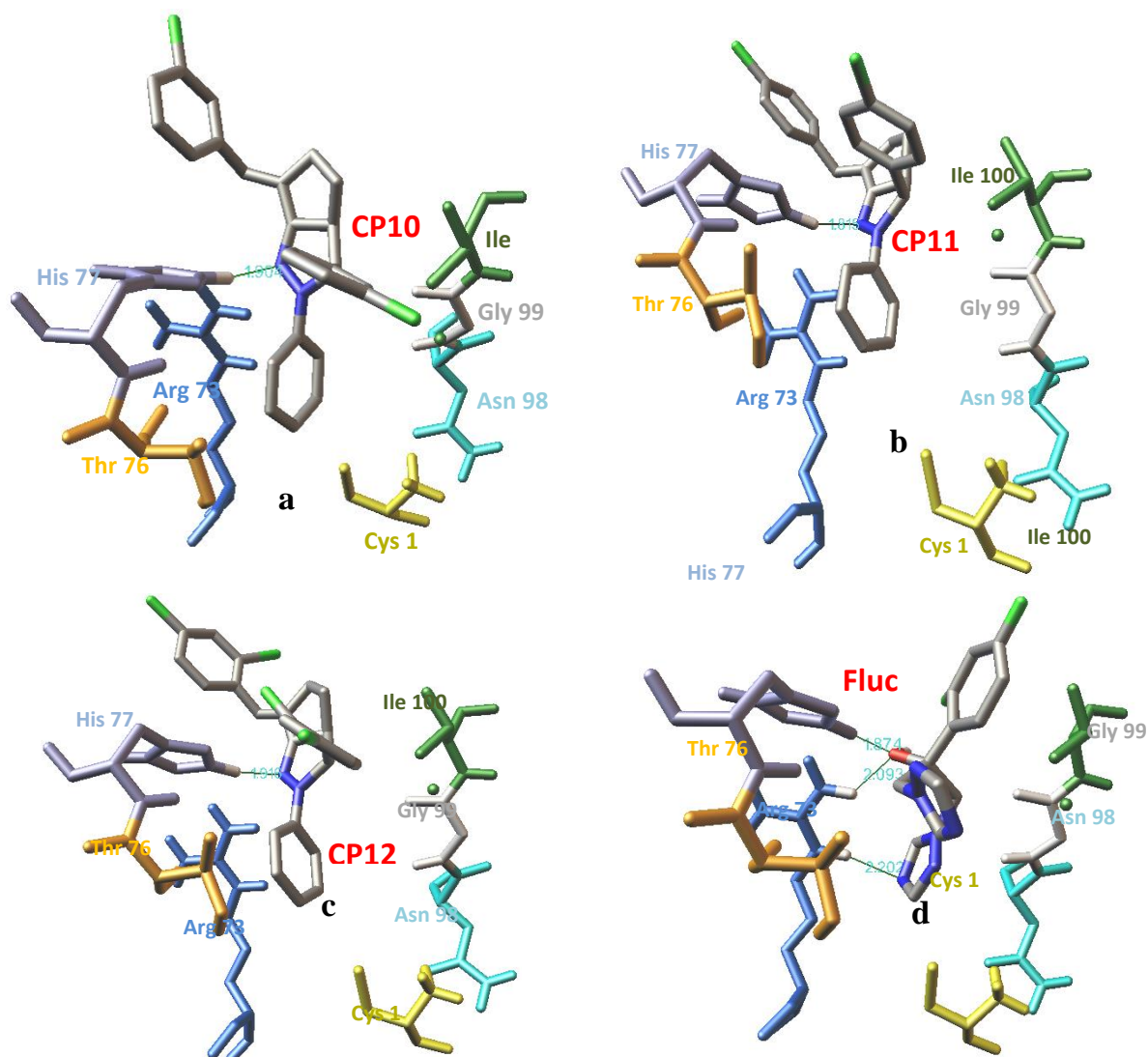
Figure 6.6: Comparative docking of pyrazole analogues of curcumin and flucanozole with (Ball and Stick model) glucosamine-6-phosphate synthase showing hydrogen bond formation within the active site 1 (**a**) compound **CP10**, (**b**) compound **CP11**, (**c**) compound **CP12**, (**d**) Flucanozole (In active site 2 no hydrogen bonds are formed).

This effect is caused by specific physical supra molecular interactions with a set of amino acid side-chains, may be ion-charge or dipole interactions, charge transfers, and

hydrophobic or hydrophilic interactions. The electronegative nucleus of the chlorine connected to a carbon atom withdraws electrons from other parts of the molecule, thus strongly polarizing that bond causing a dipole moment. A significant number of drugs and drug candidates in clinical development are halogenated structures. The formation of halogen bonds in ligand-target complexes is recognized as a kind of intermolecular interaction that favorably contributes to the stability of protein-ligand complexes.

The insertion of halogen atoms has been used in innumerous cases of hit-to-lead or lead-to-drug conversions [Buchini *et al.*2008, Bonnefous *et al.*2009, Leite *et al.*2007]. The incorporation of halogen atoms increase membrane permeability, improve the oral absorption and skin penetration [Gentry *et al.* 1999].

In the present study, the molecular docking results of compound CP10, CP11 and CP12 showed very good binding energy and RMSD, even in *in vitro* studies these analogues showed promising activity against all tested microorganisms. So it can be considered that the activity may be due to the inhibition of enzyme GlcN-6-Psynthase, which catalyses a complex reaction involving ammonia transfer from L-glutamine to Fru-6-P followed by isomerisation of the formed fructosamine-6-phosphate to glucosamine-6-phosphate.

6.5.Quantitative structure activity relatioship (QSAR) study of Synthesized Compounds

6.5.1 Quantitative structure activity relatioship (QSAR) study

The series of compounds synthesized were subjected to molecular modelling via QSAR studies using CS Chem-Office 6.0. There sequential multiple linear regression analysis was performed using in-house program VALSTAT. All equations were further validated by most popular leave one out (LOO) cross-validation method to ensure their robustness. Various equations were obtained but the following statistically significant equations with high correlation coefficient were selected.

When data set was subjected to sequential multiple linear regression analysis, in order to develop QSAR between antimicrobial activity as dependent variables and substituent constants as independent variables, several equations were obtained. The statistically significant equations were considered as best model.

Model: 1

pMIC = Probe [20.03(± 127.912)] +PMI-X [0.0001 (± 9.55435e-005)] +Tot [-6.6895(± 66.1256)] +CC [6.70457(± 66.1997)]

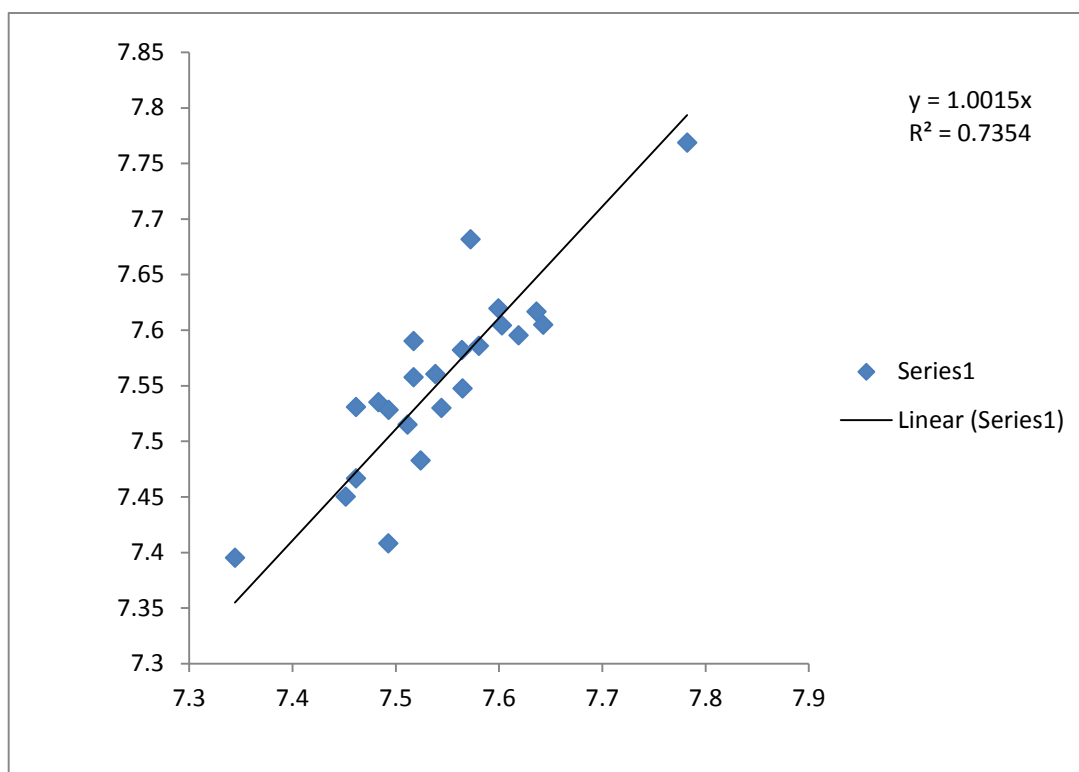n=23,r=0.832,r^2=0.735,std=0.058,F=41.8868,r^2bs =0.710, q2=0.608006,Spress=0.177856, SDEP =0.161652

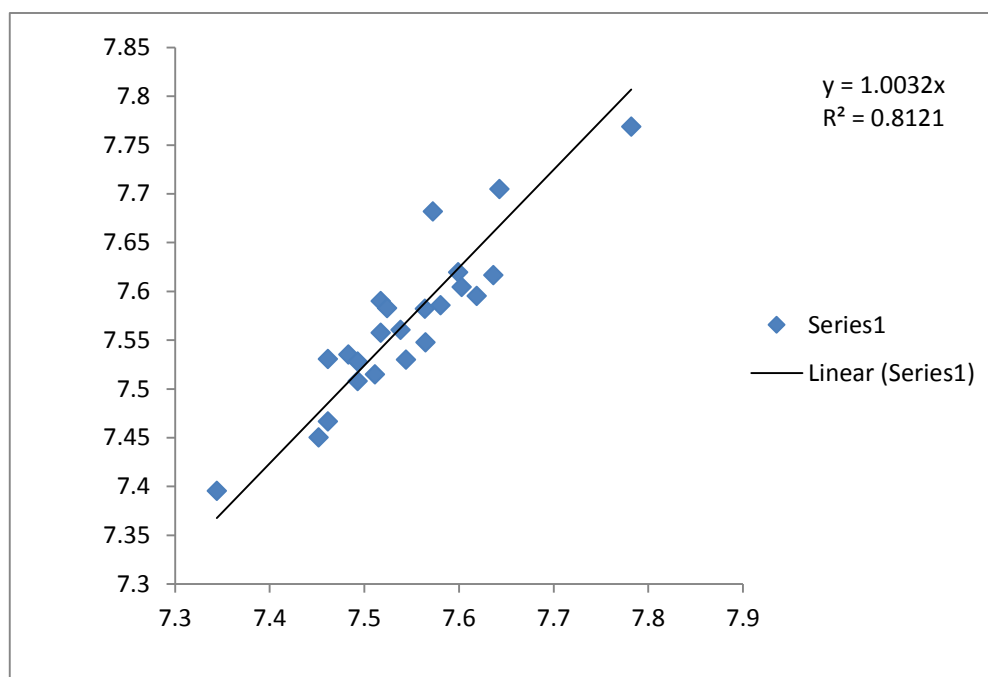**Figure 6.7:** For model 1: between the observed value of biological activity on x-axis v/s Predicted value of biological activity on Y-axis.

Model: 2

The study revealed that Repulsion energy (Electronic parameter), Molecular weight, cluster count and Molecular topological index (Steric parameter) contributed towards the inhibitory activity. The model 2 shows that steric parameter (Ovality) shows positive contribution and electronic parameters (LUMO energy and dipole moment) show negative contribution towards the activity. An accurate mathematical model was developed for predicting their inhibitory activity of curcumin analogues. The value of boot strapping r^2bs =0.80 shows that model 2 is robust. The model once again favored by the least SPRESS and SDEP values.

Contribution of molecular weight and cluster count negatively shows that as molecular weight of compound increases their activity decreases. Repulsion energy is electronic descriptors.

pMIC= MW[-23.075($\pm$ 113.83)]+ LUMO [-0.0001($\pm$ 8.2578)]+ Tot [15.423($\pm$ 58.8521)] +CC [-15.4341($\pm$ 58.9197)]

n=23,r=0.903,r^2=0.812, std=0.0534,F=51.7413, r^2bs= 0.806264, q^2= 0.71407, Spress = 0.205587, SDEP= 0.186857

Figure6.8: For model 2: between the observed value of biological activity on x-axis v/s Predicted value of biological activity on Y-axis.

Table6.16 Statistics of Significant Equations.

Model No.	n	r^2	F	r^2_{bs}	Chance	S_{DEP}	S_{PRESS}	q^2
1	23	0.73	41.886	0.71	<0.001	0.161	0.177	0.60
2	23	0.81	51.741	0.80	<0.001	0.186	0.2055	0.71

The repulsion energy (Ev) is defined as the total core-core internuclear repulsion between satoms. As the result if total repulsion energy increases their activity also increases.

Figure 6.9: ^{1}H NMR spectra of *(E)-1-(7-benzylidene-3-phenyl-3,3a,4,5,6,7-hexahydro-2H-indazol-2-yl) ethanone* (A1)

Figure 6.10: ^{13}C NMR of spectra *(E)-1-(7-benzylidene-3-phenyl-3,3a,4,5,6,7-hexahydro-2H-indazol-2-yl) ethanone* (A1)

Original Data Path: 12I30JAN2501300603_115702.RAW
Current Data Path: C:\Data2012\JAN12\
Sample ID: M-1
Acquisition Date: 1/30/2012 I3:58:25 PM
Vial: A:25
12I30JAN2501300603_115702 #45-140 RT: 0.80-1.81 AV: 96 SB: 1 0.00 NL: 1.23E7
T: + c ESI Full ms [50.00-500.00]
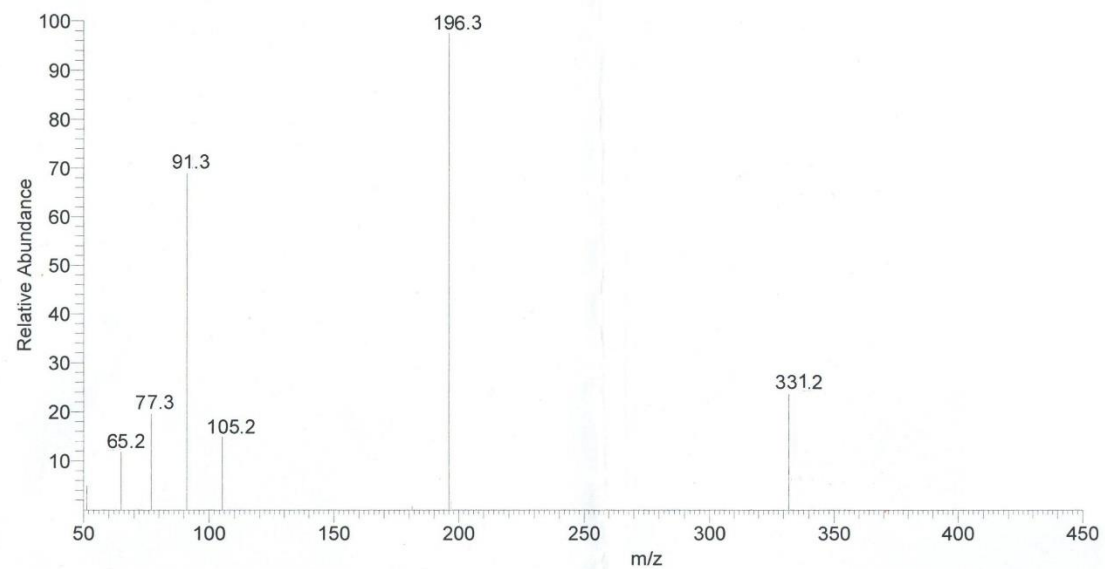
Figure 6.11: Mass spectra of *(E)-1-(7-benzylidene-3-phenyl-3,3a,4,5,6,7-hexahydro-2H-indazol-2-yl)ethanone* (A1)
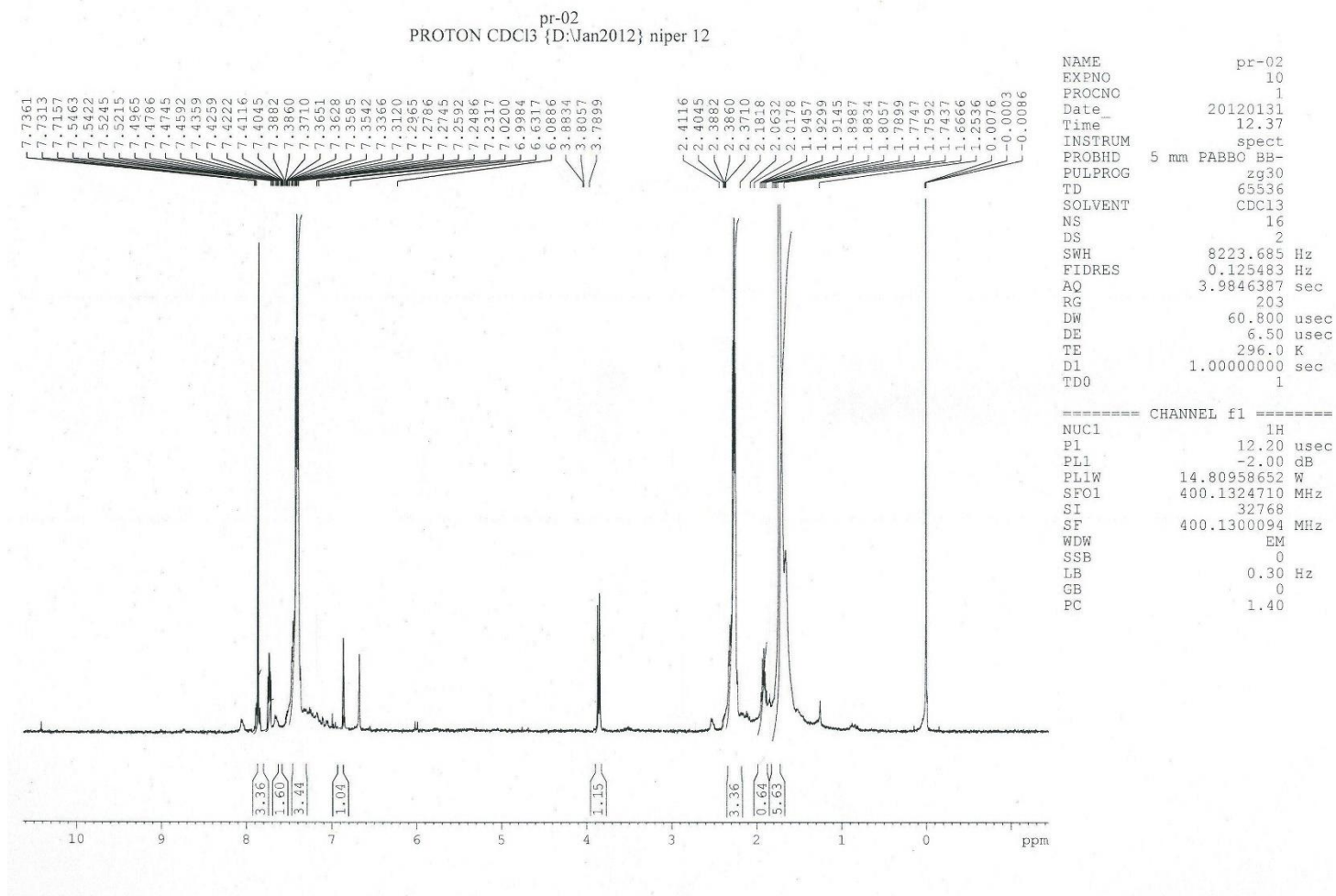
Figure 6.12: ^{1}H NMR spectra of *(E)-1-(7-(4-chlorobenzylidene)-3 -(4-chlorophenyl)- 3,3a,4,5,6,7-hexahydro-2H-indazol-2-yl)ethanone*(A4)

Original Data Path: 12I30JAN2501300603_115702.RAW
Current Data Path: C:\Data2012\JAN12\
Sample ID: M-12
Acquisition Date: 1/30/2012 12:12:25 PM
Vial: A:25
12I30JAN2501300603_115702 #45-140   RT: 0.80-1.81   AV: 96   SB: 1 0.00   NL: 1.23E7
T: + c ESI Full ms [50.00-500.00]
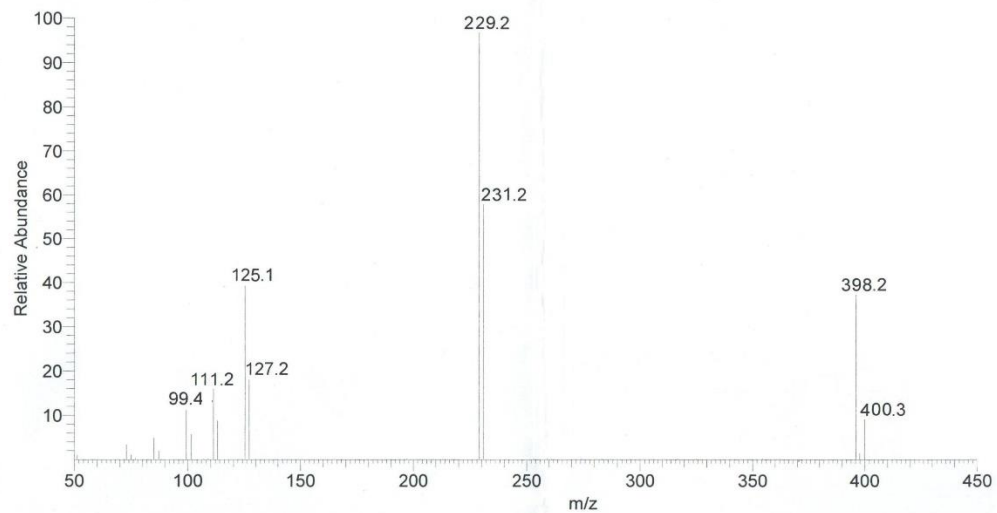
Figure 6.13: Mass spectra of *(E)-1-(7-(4-chlorobenzylidene)-3 -(4-chlorophenyl)- 3,3a,4,5,6,7-hexahydro-2H-indazol-2 yl)ethanone*(A4)
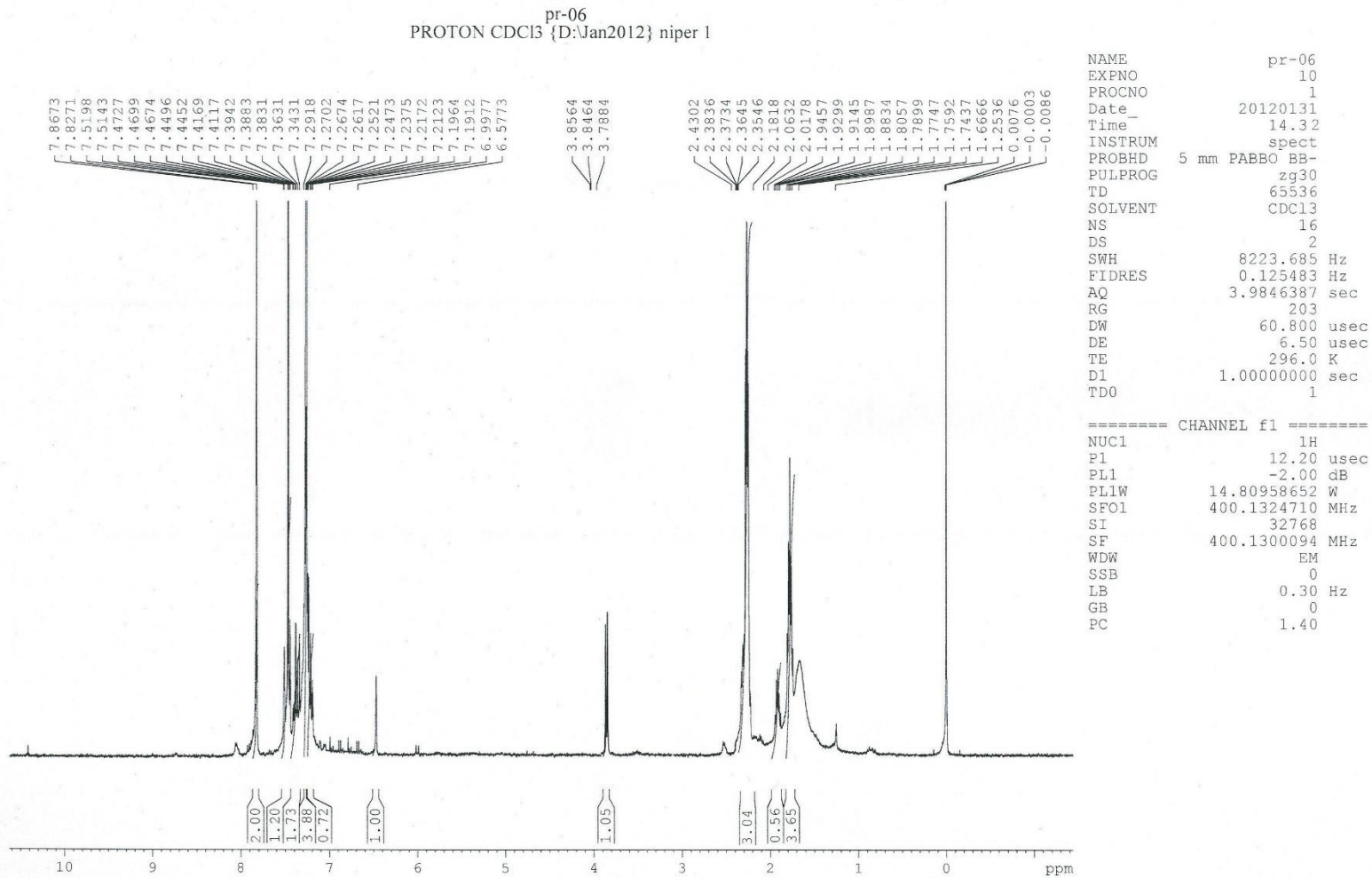
Figure 6.14: ¹H NMR spectra of *(E)-1-(6-benzylidene-3-phenyl-3a,4,5,6, tertrahydro cyclopenat [c]pyrazol-2(3H)-yl) ethanone* (CP1)
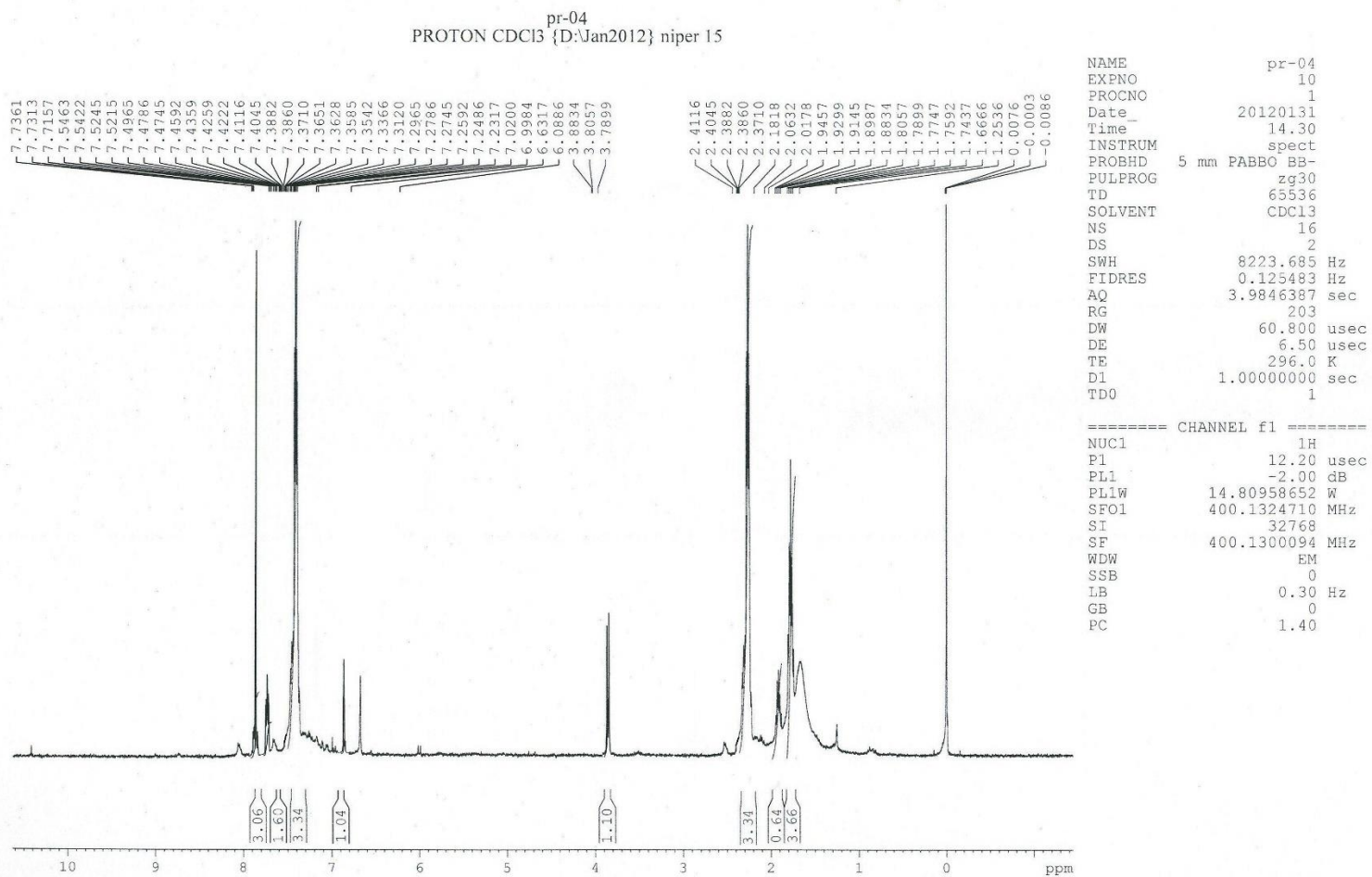
Original Data Path: 12I30JAN2501300603_115702.RAW
Current Data Path: C:\Data2012\JAN12\
Sample ID: M-5
Acquisition Date: 1/30/2012 12:28:22 PM
Vial: A:25
12I30JAN2501300603_115702 #45-140   RT: 0.80-1.81   AV: 96   SB: 1 0.00   NL: 1.23E7
T: + c ESI Full ms [50.00-500.00]
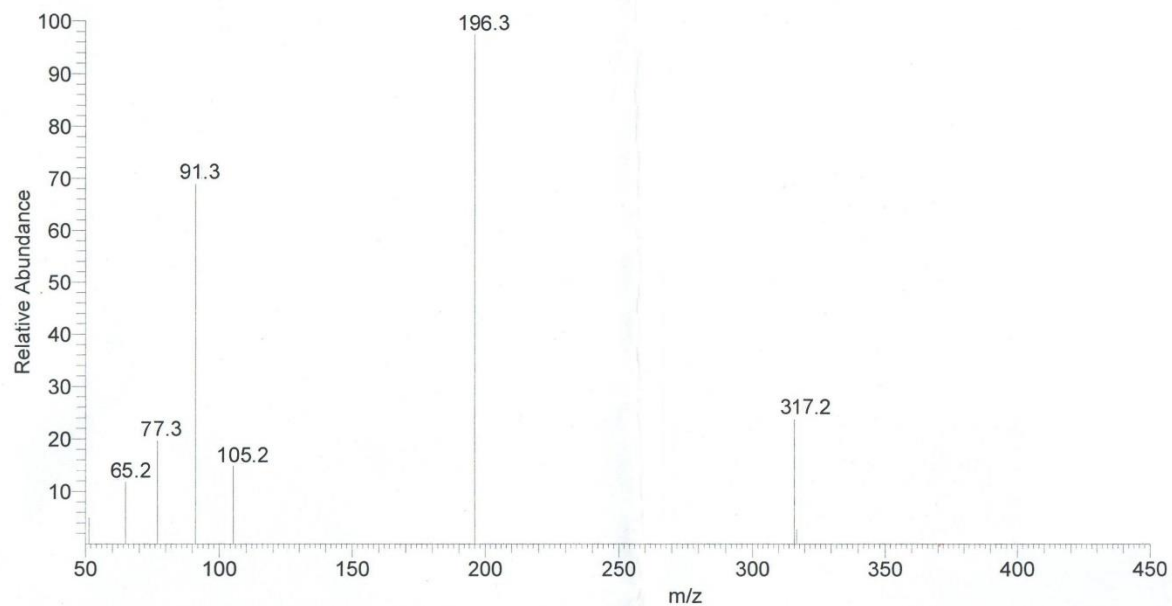
Figure 6.15: Mass spectra of *(E)-1-(6-benzylidene-3-phenyl-3a,4,5,6, tertrahydro cyclopenat [c]pyrazol-2(3H)-yl) ethanone* (CP1)

Figure 6.16: FT-IR spectra of *(E)-1-(6-benzylidene-3-phenyl-3a,4,5,6, tertrahydro cyclopenat [c]pyrazol-2(3H)-yl) ethanone* (CP1)
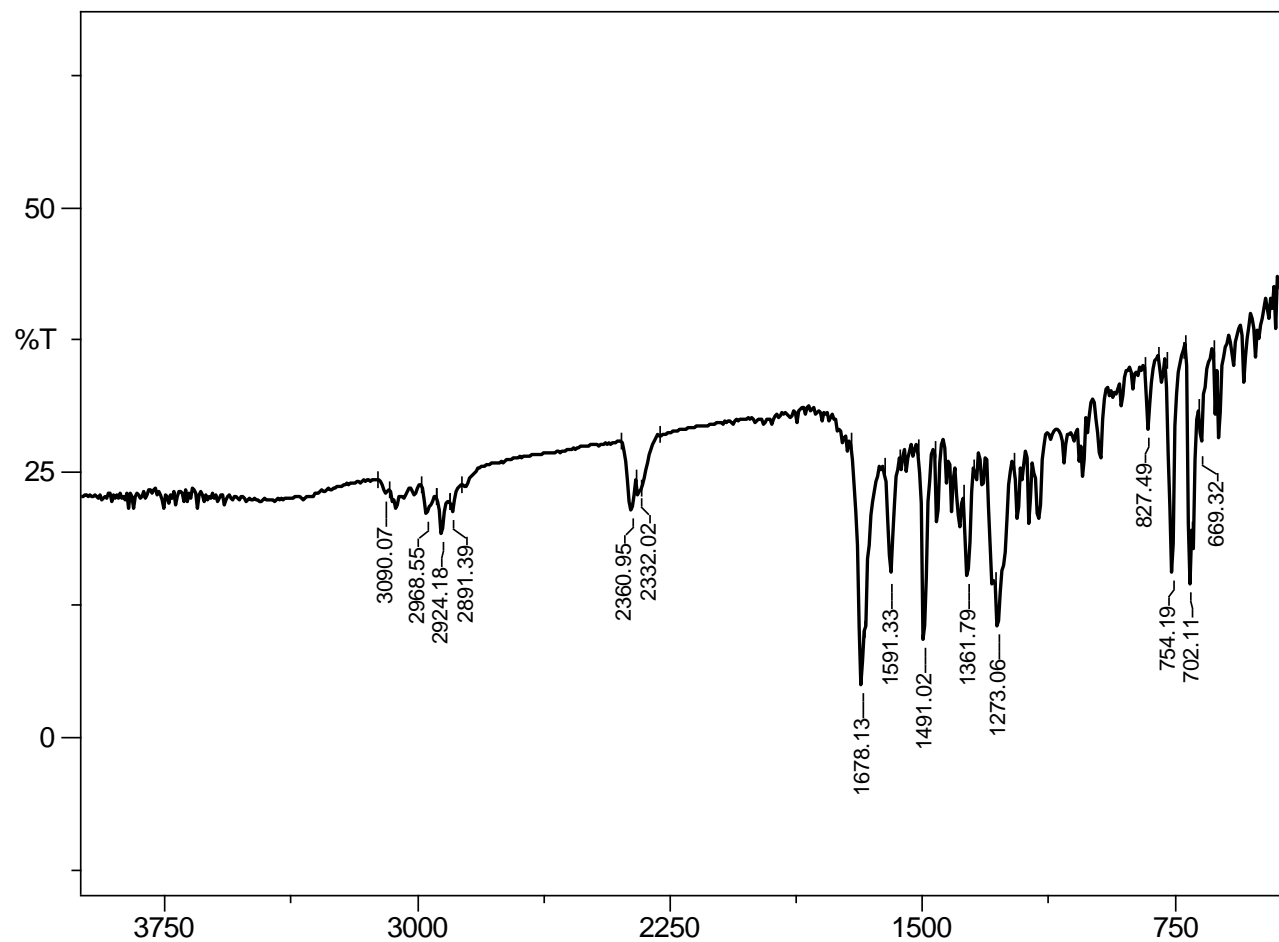
Figure 6.17: ^{1}H NMR spectra of *(E)-1-(6(4-chlorobenzylidene-3-(4-chloroyphenyl)-3a,4,5,6-tetrahydrocyclopenata[c]pyrazol-2(3H)-yl)ethanone* (CP4)

Original Data Path: 12I30JAN2501300603_115702.RAW
Current Data Path: C:\Data2012\JAN12\
Sample ID: M-6
Acquisition Date: 1/30/2012 12:58:25 PM
Vial: A:25
12I30JAN2501300603_115702 #45-140 RT: 0.80-1.81 AV: 96 SB: 1 0.00 NL: 1.23E7
T: + c ESI Full ms [50.00-500.00]
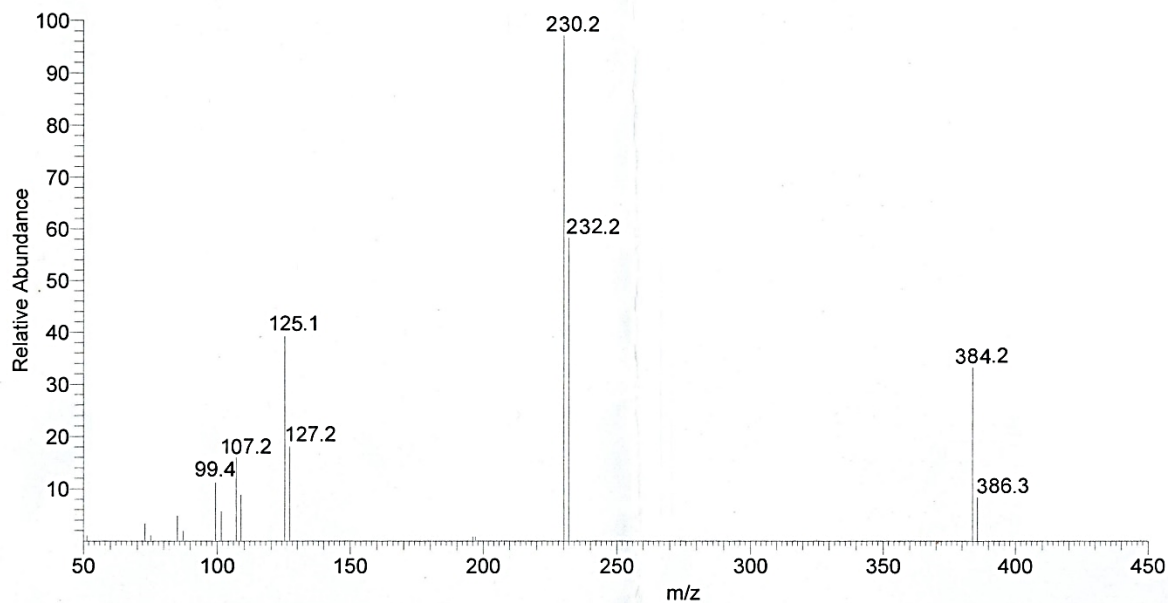
Figure 6.18: Mass spectra of *(E)-1-(6(4-chlorobenzylidene-3-(4-chloroyphenyl)-3a,4,5,6-tertrahydrocyclopenata[c]pyrazol-2(3H)-yl)ethanone* (CP4)

Figure 6.19: FT-IR spectra of *(E)-1-(6(4-chlorobenzylidene-3-(4-chloroyphenyl)-3a,4,5,6-tertrahydrocyclopenata[c]pyrazol-2(3H)-yl)ethanone* (CP4)
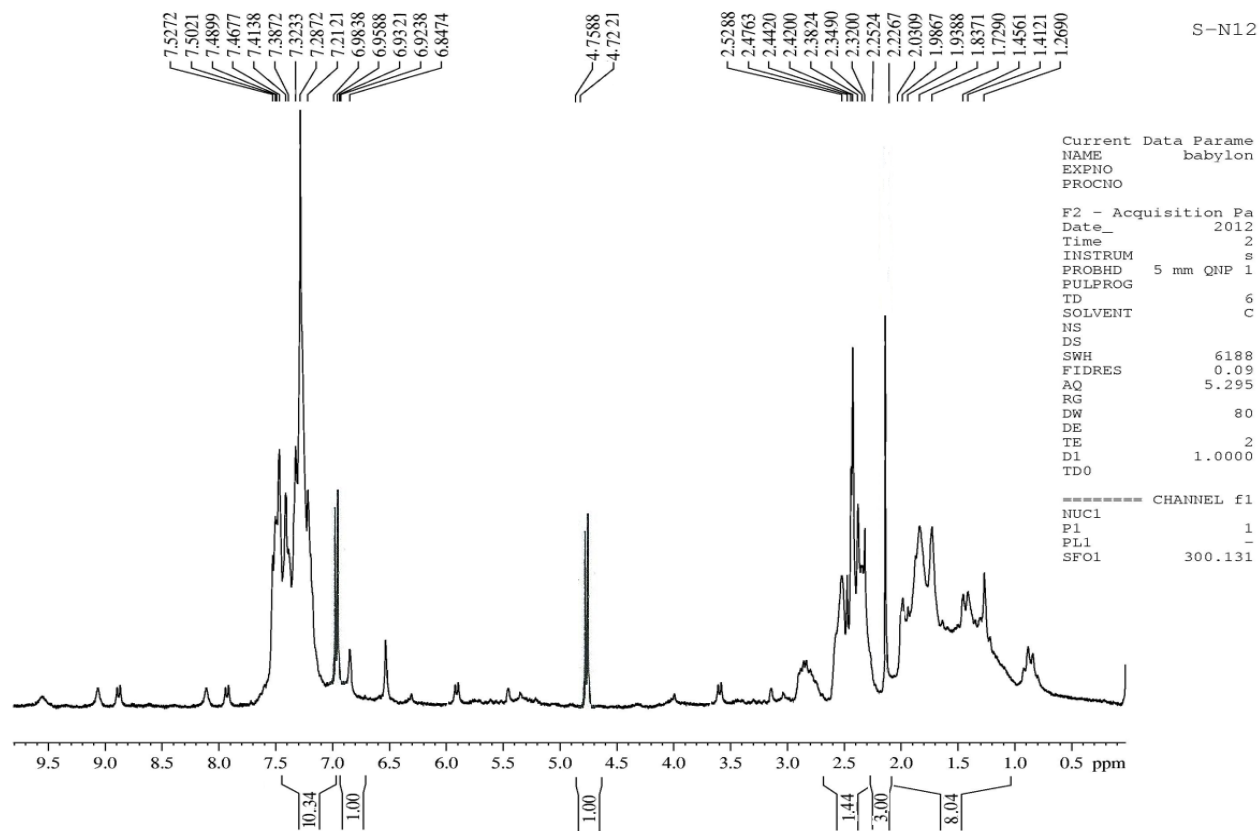
Figure 6.20: ^{1}H NMR spectra of *(E)-1-(8-benzylidene-3-phenyl-3a,4,5,6,7,8-hexahydro cyclohepta [c]pyrazol-2(3H)-yl)ethanone* (C1)

Original Data Path: 12I30JAN2501300603_115702.RAW
Current Data Path: C:\Data2012\JAN12\
Sample ID: M-8
Acquisition Date: 1/30/2012 12:11:25 PM
Vial: A:25
12I30JAN2501300603_115702 #45-140 RT: 0.80-1.81 AV: 96 SB: 1 0.00 NL: 1.23E7
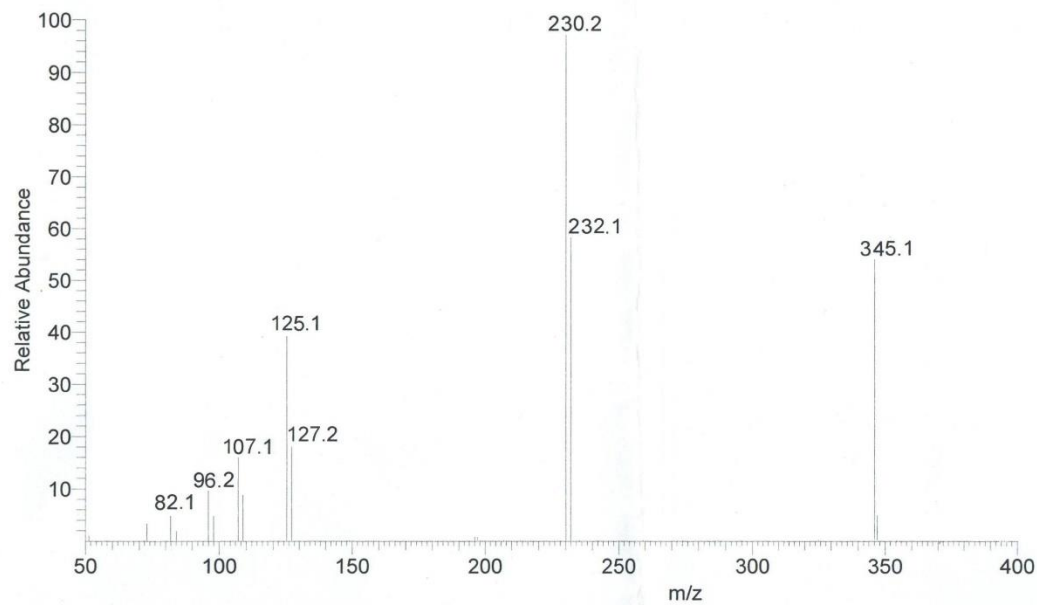T: + c ESI Full ms [50.00-500.00]

Figure 6.21: Mass spectra of of *(E)-1-(8-benzylidene-3-phenyl-3a,4,5,6,7,8-hexahydro cyclohepta [c]pyrazol-2(3H)-yl)ethanone* (C1)
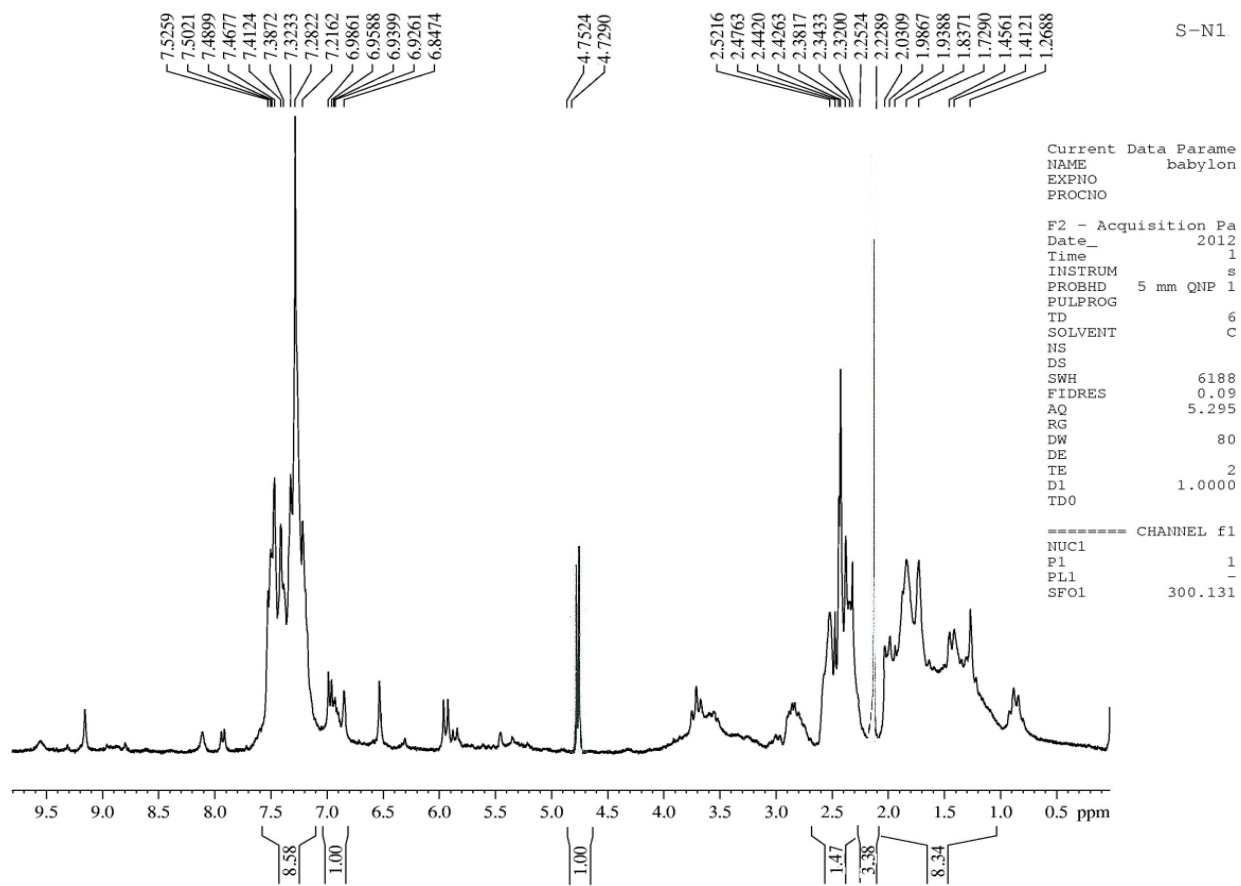
Figure 6.22: ^{1}H NMR spectra of (E)-1-(8-(2-chlorobenzylidene)-3-(2-chlorophenyl)-3a,4,5,6,7,8-hexahydro cyclohepta[c]pyrazol-2(3H)-yl)ethanone (C2)

Original Data Path: 12I30JAN1501300593_115046.RAW
Current Data Path: C:\Data2012\JAN12\
Sample ID: M-4
Acquisition Date: 1/30/2012 12:25:56 PM
Vial: A:15

12I30JAN1501300593_115046 #48-131 RT: 0.81-1.81 AV: 84 SB: 1 0.00 NL: 7.42E5
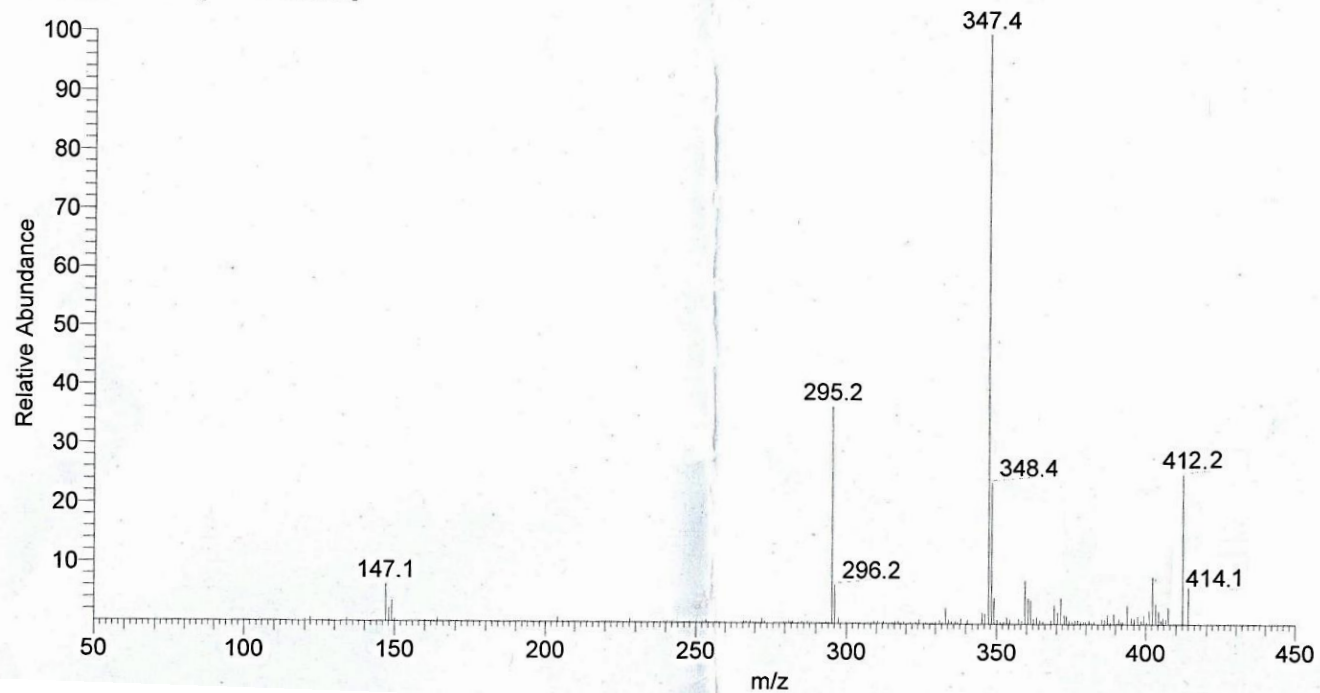T: + c ESI Full ms [50.00-500.00]

Figure 6.23: Mass spectra of of *(E)-1-(8-(2-chlorobenzylidene)-3-(2-chlorophenyl)-3a,4,5,6,7,8-hexahydrocyclohepta[c]pyrazol-2(3H)-yl)ethanone* (C2)